

Escola Politécnica da Universidade de São Paulo
STELLA LEE

**The Effect of Alloying Elements on Critical Transformation Temperatures and
NbC precipitation in Tempered Bainite in Medium Mn Steels**

São Paulo
2018

Escola Politécnica da Universidade de São Paulo

STELLA LEE

**The Effect of Alloying Elements on Critical Transformation Temperatures and
NbC precipitation in Tempered Bainite in Medium Mn Steels**

Trabalho de Formatura apresentado à Escola
Politécnica da Universidade de São Paulo
como requisito à obtenção do título de
Engenheira

Orientador: Prof. Dr. Hélio Goldenstein

São Paulo

2018

Escola Politécnica da Universidade de São Paulo

STELLA LEE

**The Effect of Alloying Elements on Critical Transformation Temperatures and
NbC precipitation in Tempered Bainite in Medium Mn Steels**

Trabalho de Formatura apresentado à Escola
Politécnica da Universidade de São Paulo
como requisito à obtenção do título de
Engenheira

Área de Concentração: Engenharia
Metalúrgica e de Materiais

Orientador: Prof. Dr. Hélio Goldenstein

São Paulo

2018

Autorizo a reprodução e divulgação total ou parcial deste trabalho, por qualquer meio convencional ou eletrônico, para fins de estudo e pesquisa, desde que citada a fonte.

TF-2018

LS15 e

2304753

H 2018 0

DEDALUS - Acervo - EPMT



31800009342

Catalogação-na-publicação

Lee, Stella

The Effect of Alloying Elements on Critical Transformation Temperatures and NbC precipitation in Tempered Bainite in Medium Mn Steels / S. Lee -- São Paulo, 2018.

53 p.

Trabalho de Formatura - Escola Politécnica da Universidade de São Paulo. Departamento de Engenharia Metalúrgica e de Materiais.

1.AÇO DE ALTA RESISTÊNCIA 2.AÇO BAIXO CARBONO
3.TRANSFORMAÇÕES DE FASE I.Universidade de São Paulo. Escola Politécnica. Departamento de Engenharia Metalúrgica e de Materiais II.t.

Dedico este trabalho à minha família, aos
meus professores e aos meus amigos.

AGRADECIMENTOS

Ao meu orientador Prof. Dr. Hélio Goldenstein por toda a paciência, compreensão e apoio que me ofereceu ao longo da minha graduação, além de ser o grande responsável pela minha ida à França, onde pude realizar o estágio que deu origem ao presente trabalho.

Aos meus coorientadores Prof. Dr. Laerte Idal Sznelwar e Prof. Dra. Roseli de Deus Lopes por acreditarem na minha capacidade e me oferecerem apoio sempre que necessitei. Serei eternamente grata por terem me proporcionado grandes aprendizados e muito crescimento como ser humano.

Aos Professores Dr. Fernando Landgraf, Dra. Ivette Frida Oppenheim, Dr. Samuel Toffoli e Dr. Guilherme Lenz pelo carinho e dedicação que têm com seus alunos. Agradeço pelas inúmeras chances que me proporcionaram e por não me deixarem desistir.

A todos os funcionários do PMT pelo ótimo trabalho e pela simpatia.

Ao Engenheiro Ian Zuazo, meu tutor durante o estágio na Arcelor Mittal, por ter me proporcionado grandes aprendizados na área técnica, pela paciência e pela amizade ao longo de um ano na França.

À Arcelor Mittal pela oportunidade única e inesquecível que deu fruto ao presente trabalho e por permitirem o uso de dados, informações e pesquisas pertencentes à empresa.

A todos os meus colegas e amigos que me apoiaram e me motivaram durante a minha longa graduação e durante minha vida. Agradecimentos especiais a Hugo Hashimoto, Renato Ito, Fernando Kameoka, Gustavo Suto, Bruna Fernandes, Ligia Doyama, Prof Dr. Eduardo Monlevade, Prof Dr. Jorge Tenório, Mariana Amemiya, Érika Rossi, Renate Fukunaga, Mauro Fukunaga, Reinaldo Yonamine, Claudio Brunoro, Maud Eikoff, Fabiana Raulino, Elena Saggio, Irene Ficheman, Wesley Cheng, Jack Yoshida, Anne Hung, Renata Kotaira, Valéria Goto e Xuan Wen.

À equipe de basquete feminino da Poli, minha segunda família na graduação, a quem atribuo a minha permanência na faculdade, as minhas melhores experiências durante a graduação e grandes aprendizados de vida.

À Escola Politécnica da Universidade de São Paulo.

À Dra. Magda por me ajudar a superar diversos bloqueios mentais e emocionais, a lidar com os meus medos e, principalmente, por me ensinar a aceitar e respeitar a mim mesma como sou.

Agradeço a minha família por sempre me apoiar, torcer pelo meu sucesso e me amar incondicionalmente.

Agradeço especialmente ao Wagner, pois o seu apoio e sua compreensão nestes últimos anos foram fundamentais para que eu pudesse superar grandes dificuldades e me tornar uma pessoa melhor.

Sem seguir nenhuma religião em específico, agradeço a algo infinitamente maior do que eu, a grande energia do Universo que nos permite a vida, a quem muitos chamam de "Deus". Eu simplesmente chamo de amor e luz.

Cheguei até aqui graças a todos que fazem ou fizeram parte da minha vida.

Desejo muito amor e muita luz a todos. Muito obrigada!

"Our greatest weakness lies in giving up.

The most certain way to succeed is always to try just one more time."

Thomas Edison

RESUMO

A cada ano, o Centro Global de Pesquisa e Desenvolvimento da Arcelor Mittal, em Maizi  re-les-Metz, na Fran  a, recruta estudantes de todo o mundo para seu programa de est  gio em P&D. Como uma de suas estagi  rias, tive a oportunidade de trabalhar com engenheiros e t  cnicos de P&D muito experientes e, atrav  s de experi  ncias pr  ticas, ampliar o conhecimento pr  vio em metalurgia f  sica e transforma  es de fase que eu tive durante a minha gradua  o em Engenharia de Materiais. Al  m disso, obtive experi  ncia pr  tica com dilatometria, procedimentos e an  lises metalogr  ficos, prepara  o de amostras e an  lises para MEV e MET e, consequentemente ampliei minha vis  o sobre a \'rea da metalurgia. Esta pesquisa foi parte de um programa de P&D da Arcelor Mittal em parceria com a CBMM (Companhia Brasileira de Metalurgia e Minera  o), cujo objetivo era estudar, por meio de temperaturas cr  ticas, transforma  o de fase e propriedades mec  nicas os efeitos de alguns elementos de liga, como o mangan  s e o sil  cio, na precipita  o de part  culas ricas em ni  bio. O objetivo   lcan  ar maiores resist  ncias em a  os de baixo carbono microligados com Nb, amplamente utilizados em ind  strias automotivas. Amostras de ligas de mangan  s m  dio com diferentes teores de Nb e Si foram submetidas a diferentes tratamentos t  rmicos utilizando um dilat  metro. Temperaturas cr  ticas e microestruturas foram analisadas por m  todos convencionais. O papel do Mn expandindo o campo da austenita foi explorado para   lcan  ar uma maior dissolu  o de Nb. O Nb, por outro lado, mostrou n  o ter uma grande influ  ncia na cin  tica de form  a  o da bainita, quando as amostras foram mantidas isotermicamente a 400 ° C. A adi  o de Si retardou significativamente a cin  tica de transforma  o. Mesmo assim, parece aumentar a dureza ap  s a precipita  o de carbonetos, sendo mais eficiente quando revenido por periodos curtos.    poss  vel que a natureza dessa maior for  a se deva    martensita originada da austenita que n  o se transformou.

Palavras-chave: Arcelor Mittal, dilatometria, m  dio-mangan  s, temperatura cr  tica, in  cio de transforma  o martens  tica, transforma  o bain  tica.

ABSTRACT

Each year Arcelor Mittal Global R&D Centre in Maizi  re-les-Metz, France, recruits students from all over the world for their R&D internship program. As one of their interns, I was able to work closely with very experienced R&D engineers and technicians, learn physical metallurgy and phase transformations through practical experiences in additions to the previous knowledge I had from my Materials Science undergraduate background, gain hands-on experience with dilatometry, metallographic procedures and analysis, follow sample preparations and analysis for SEM and TEM, and also enhance my understanding of the metallurgical field. This investigation is part of a partnership R&D program between Arcelor Mittal and CBMM (Companhia Brasileira de Metalurgia e Minera  o). The aim was to study the effects of some alloying elements, such as Manganese and Silicon, on the precipitation of Niobium-rich particles by the means of critical temperatures, phase transformation and mechanical properties, in order to achieve higher strengths in low carbon steels microalloyed with Nb, largely used in automotive industries. Medium Manganese alloy samples with different contents of Nb and Si were submitted to different heat treatments using a dilatometer. Critical temperatures and microstructures were analyzed by conventional methods. The role of Mn by expanding the austenite field was explored to achieve a great Nb dissolution. This latter showed to not have a major influence on the bainite formation kinetics when specimens were held isothermally at 400  C. The addition of Si retarded significantly the transformation kinetics. Even so, it appears to favor strength after carbide precipitation, this latter being more efficient when tempering was performed for very short times. Nevertheless, it is possible that the nature of this higher strength is due to the martensite originated from the austenite that didn't transform into bainite.

Keywords: Arcelor Mittal, dilatometry, medium manganese, critical temperature, martensite-start, bainite formation.

LIST OF FIGURES

FIGURE 1 – FE-C PHASE DIAGRAM AT DIFFERENT TEMPERATURES. SOURCE: [3].	18
FIGURE 2 – TTT CURVES SHOWING THE DIFFERENT DOMAINS OF TRANSFORMATION. SOURCE: [4].	20
FIGURE 3 – DIAGRAMS OF ISOTHERMAL TRANSFORMATION: (A) CARBON STEEL AND STEEL ALLOYED WITH NON-CARBIDE-FORMING ELEMENTS; (B) CARBON STEEL AND STEEL ALLOYED WITH CARBIDE-FORMING ELEMENTS [5].	23
FIGURE 4 – ISOTHERMAL TRANSFORMATION DIAGRAMS SHOWING THE EFFECT OF INCREASING AMOUNTS OF MN ON THE COOLING RATES. SOURCE: [5].	24
FIGURE 5 – SOLUBILITY PRODUCT OF CARBIDES AND NITRIDES IN AUSTENITE AS A FUNCTION OF TEMPERATURE [6]	25
FIGURE 6 – EFFECT OF MN ON THE SOLUBILITY PRODUCT OF NBC IN AUSTENITE. SOURCE: [7].	27
FIGURE 7 – A3 INFLUENCE OF MN SOLUBILITY OF NBC IN AUSTENITE. SOURCE: [7].	28
FIGURE 8 – EFFECT OF SI ON THE SOLUBILITY PRODUCT OF NBC IN AUSTENITE. SOURCE: [7].	28
FIGURE 9 – (A-D) 3MN (NITAL) AND (E-H) 5MN (PICRAL + METABISULFITE) WITH 0NB, 0.05NB, 0.1NB AND 0.1NB-1.5SI. ADDITIONS OF MN AVOID FERRITE AND PEARLITE FORMATION DURING AIR COOLING AFTER HOT ROLLING. SI ADDITIONS INCREASES MORE HARDENABILITY.	31
FIGURE 10 – THERMAL TREATMENT CYCLE: AUSTENITIZING AT 1250°C FOR 5 MINUTES FOLLOWED BY QUENCHING (~50°C/S)	32
FIGURE 11 - FERRITE TO AUSTENITE TRANSFORMATION DURING HEATING IN A DILATATION CURVE	32
FIGURE 12 - TANGENT LINES TRACED AT THE BEGINNING AND AT THE END OF A \rightarrow F TRANSFORMATION	33
FIGURE 13 - MARTENSITE TRANSFORMATION DURING QUENCHING IN A DILATATION CURVE.	33
FIGURE 14 - TANGENT LINES AT THE BEGINNING AND AT THE END OF MARTENSITE TRANSFORMATION.	34
FIGURE 15 – GRAPH SHOWING THE MARTENSITE VOLUME FRACTION AS A FUNCTION OF TEMPERATURE DURING MARTENSITE TRANSFORMATION UPON QUENCHING.	35
FIGURE 16 - KOISTENEN & MARBURGER FITTED TO TRANSFORMED MARTENSITE VOLUME FRACTION FOR MS1 ESTIMATION.	36
FIGURE 17 - GRAPH ILLUSTRATING MS2 ESTIMATION.	36
FIGURE 18 – THERMAL CYCLE FOR BAINITE FORMATION.	37
FIGURE 19 – BAINITE TEMPERING CYCLES	38
FIGURE 20 – THE EFFECT OF DIFFERENT CONCENTRATIONS OF MN ON AC1 AND AC3.	39
FIGURE 21 – THE EFFECT OF DIFFERENT AMOUNTS OF SI ON AC1 AND AC3.	40
FIGURE 22 – THE EFFECT OF DIFFERENT CONCENTRATIONS OF MN ON 0%NB-1.5%SI SAMPLES.	40
FIGURE 23 – THE EFFECT OF MN ON CRITICAL TEMPERATURES, AC1 AND AC3, OF SAMPLES THAT VARY IN NB AND SI CONCENTRATIONS.	41
FIGURE 24 – A COMPARISON OF THE EFFECT OF MN ON MARTENSITE-START TEMPERATURE (MS) WITH DIFFERENT SI CONCENTRATIONS IN 0.1%NB SAMPLES CALCULATED BY USING 4 DISTINCT METHODS : THE PRESENT STUDY, ANDREWS, ISHIDA, AND MAHIEU.	42

FIGURE 25 – DILATOMETRY CURVES DURING MARTENSITE TRANSFORMATION FOR DIFFERENT CONTENTS OF MN. A) EFFECT OF MN ON THE MS TEMPERATURE; B) EFFECT OF MN ON THE KINETICS OF TRANSFORMATION.	43
FIGURE 26 – THE EFFECT OF MN ON THE MS OF SAMPLES WITH DIFFERENT NB CONCENTRATIONS.	43
FIGURE 27 – THE EFFECT OF NB ON THE MS OF SAMPLES WITH DIFFERENT MN CONCENTRATIONS.	44
FIGURE 28 – DILATOMETRY CURVES DURING MARTENSITE TRANSFORMATION FOR DIFFERENT CONTENTS OF NB IN SAMPLES WITH 3%MN-0%SI.	45
FIGURE 29 – DILATOMETRY CURVES DURING MARTENSITE TRANSFORMATION FOR DIFFERENT CONTENTS OF SI IN SAMPLES WITH 3%MN-0.1%NB.	45
FIGURE 30 – THE EFFECT OF MN ON THE MS OF SAMPLES WITH DIFFERENT SI CONCENTRATIONS.	46
FIGURE 31 – A COLUMN GRAPHIC SHOWING THE EFFECT OF MN ON THE MS OF SAMPLES WITH DIFFERENT SI CONCENTRATIONS.	46
FIGURE 32 – THE EFFECT OF DIFFERENT NB AND SI CONCENTRATIONS ON BAINITE FORMATION KINETICS. SAMPLES WERE AUSTENITIZED FOR 5 MINUTES AND QUENCHED TO 400°C FOR BAINITE FORMATION, AND QUENCHED AGAIN TO ROOM TEMPERATURE AFTER 5 MINUTES.	47
FIGURE 33 – MICROSTRUCTURES OF 3MN-0.18C-(0-0.1)NB-(0-1.5)SI. SAMPLES WERE AUSTENITIZED AT 1250°C, ISOTHERMALLY TREATED AT 400°C FOR 5 MIN AND QUENCHED. PICRAL FOLLOWED BY METABISULFITE ETCHING. A) 0NB-0SI; B) 0.05NB-0SI; C) 0.1NB-0SI; D) 0.1NB-1.5SI	48
FIGURE 34 – MICROSTRUCTURES OF 3MN-0.18C-(0-0.1)NB-(0-1.5)SI. SAMPLES WERE AUSTENITIZED AT 1250°C, ISOTHERMALLY TREATED AT 400°C FOR 5 MIN, TEMPERED AT 600°C FOR 5 MIN AND QUENCHED. PICRAL FOLLOWED BY METABISULFITE ETCHING. A) 0NB-0SI; B) 0.05NB-0SI; C) 0.1NB-0SI; D) 0.1NB-1.5SI	49
FIGURE 35 – THE EFFECT OF NB AND SI ADDITIONS ON VICKERS HARDNESS MESURED AFTER BAINITE FORMATION AT 400°C/5' AND TEMPERING AT 600°C FOR DIFFERENT PERIODS OF TIME : 30'', 60'' AND 300''. THE 0'' CURVE REPRESENTS THE SAMPLES THAT WERE QUANCHED RIGHT AFTER BAINITE FORMATION AT 400°C/5'.	50
FIGURE 36 – GRAPHIC WITH COLUMNS SHOWING THE EFFECT OF NB AND SI ADDITIONS ON VICKERS HARDNESS MESURED AFTER BAINITE FORMATION AT 400°C/5' AND TEMPERING AT 600°C FOR DIFFERENT PERIODS OF TIME : 30'', 60'' AND 300''. THE 0'' COLUMN REPRESENTS THE SAMPLES THAT WERE QUANCHED RIGHT AFTER BAINITE FORMATION AT 400°C/5'.	50

LIST OF TABLES

TABLE 1 – CHEMICAL COMPOSITIONS OF SAMPLES	29
TABLE 2 - EXPERIMENTALY ESTIMATED AC1, AC3, MS (MS1) AND MS2 VALUES FOR EACH S VALU FOR EACH COMPOSITION.	38

INDEX

1	INTRODUCTION	14
2	AIM OF THE STUDY	16
3	LITERATURE REVIEW	17
3.1	PHASE TRANSFORMATION IN STEELS	17
3.1.1	Phase Diagram for the Fe-C System	18
3.1.2	Martensite Transformation.....	19
3.1.3	Bainite Formation.....	20
3.1.4	Tempering of bainite.....	20
3.2	Alloying elements in Steels	21
3.2.1	Substitutional elements	21
3.2.2	Interstitial elements	21
3.2.3	Microalloying in steels.....	22
3.2.4	Transformation Diagrams.....	23
3.2.5	Effect on TTT curves	23
3.3	High Strength Steels (HSS) and Advanced High Strength Steels (AHSS)	25
4	ChoSING the composition	27
5	MATERIALS AND EXPERIMENTAL METHODS	29
5.1	Materials	29
5.2	Experimental Methods.....	31
5.2.1	Ferrite to Austenite transformation: Ac1 and Ac3 temperatures.....	32
5.2.2	Martensite transformation: Ms temperature.....	33
5.2.3	Bainite formation	37
5.2.4	Tempering of bainite	37
6	RESULTS AND DISCUSSION	38
6.1	Effect on Ac1 and Ac3	39
6.2	Effect on Ms1	41
6.3	On bainite formation.....	46
6.3.1	Bainite Kinetics	46
6.3.2	Microstructure of the bainite.....	48
6.3.3	Vickers hardness test	49
7	CONCLUSIONS	51
8	REFERENCES	52

1 INTRODUCTION

The relevance of investing in innovation and renovation, which of course means more investments in R&D, is becoming each day more and more evident when it comes to the main multinational companies especially regarding those with industry operations. But even the concept of innovating has changed a lot in the past years. Massive production, time saving and low cost were the main goals a few years ago, whereas today a company's profit derives also from the final product quality and sustainability.

As human knowledge speeds up each day, materials science seems to be the key to new technologies and solutions to attend all sorts of demands.

Iron and its alloys play a major role in material science, especially concerning steels. From weapons in the early periods Before Christ to modern skyscrapers, steel will always be a subject with enough complexity for further studies. This involves mainly microstructures and the properties given by them. And when it comes to microstructures of steels, it becomes quite important to understand the properties and characteristics, and the mechanisms that control them such as chemical composition and particle distribution, nevertheless physical phenomenon, i.e. environmental conditions, thermal and mechanical processes. All which are parts of the core of metallurgy: phase transformations.

By understanding phase transformations, it is possible to change the whole process of steelmaking. The main parameters such as composition, temperature control, cooling/heating rates, time, external forces, etc, are the key for new materials development. These are main parameters for several studies and investigations when it comes up to optimizing the materials properties matched with a feasible industrial process, i.e. insuring the demand for the final product in a reasonable time with the lowest cost possible.

Recent studies have made great efforts on investigating the role of alloying elements in steels to control phase transformations as well as the influence of the procedures that should be undertaken with each type of composition. These elements have proven to be important when it comes to improving final properties such as weldability, formability, strength, and resistance to corrosion.

During the past recent decades sustainability has become the focus for innovation. For steel companies especially in the automobile industry this means materials with higher mechanical properties and lower weight and cost. Since then many researches and studies attempt to develop different types of steels containing such properties, as well as new processing methods. Among these advances High Strength Steels (HSS) seemed to have come to take over the leading role. Unfortunately, the gain in strength in these steels happened to be followed by considerable loss in formability. Rapidly recent studies to minimize this trade-off lead to a new generation of steels called Advanced High Strength Steels (AHSS). Nowadays automobile industries use a wide range of combinations between HSS and AHSS (as well as other types of steels, a great deal of polymers and composites) to meet the demands of a 21st Century customer.

2 AIM OF THE STUDY

This study was divided in two parts. The first aims on finding the effects of Mn and Si on critical temperatures (e.g. Ac_1 , Ac_3 and Ms) during heat treatments, hence on phase transformations. Once knowing these temperatures, it is possible to determine the range in which bainite formation occurs leading to the second part of the study, which is to observe the Mn and Si effects on the precipitation of Nb-particles during tempering after the bainite formation.

3 LITERATURE REVIEW

3.1 PHASE TRANSFORMATION IN STEELS

Steels are iron alloys containing many other chemical components. Other than iron, Carbon is a major component in many types of steel. Some of them also contain elements such as Chromium, Manganese, Niobium, etc, depending on the final use for the steel [1].

Thus, for the purpose to understand phase transformations in most of the steels, it is important to first understand the phase transformations in iron, since it is the main element and the basic structure for all the steels.

In a given system, a phase is denominated by being a portion with homogeneous properties and composition. The portions in the system differ physically. The chemical composition in a system can be distributed differently in each phase due to the different crystal structure in each one. The different phases are separated by boundaries – or interfaces. The crystal structures are the atom arrangements of minimum energy [1].

In the case of pure iron, there are two distinct phases. One is called alfa-iron phase or ferrite, which has a body centered cubic crystal (bcc) structure and is stable at temperatures from absolute zero to 912°C, the other one is the gamma-iron phase or austenite, which has a face-centered cubic crystal (fcc) structure and stable at temperatures between 912°C to 1394°C. And above this temperature, but below 1538°C (iron melting point), the bcc structure becomes stable again, except that in this case it is called delta-iron or delta-ferrite - so it can be differentiated from the alfa-iron. The bcc and fcc have basic unit cells which repeat themselves among the whole material, forming planes which also repeat themselves like parallel "sheets" of atoms. Depending on how these planes are arranged, different properties and different behaviors can appear in the iron structure including defects. The structural arrangement also affects the behavior of other elements frequently added to the steels such as carbon which at certain temperature can form iron carbide (Fe_3C), also known as cementite, an orthorhombic crystal structure and metastable phase [1].

3.1.1 Phase Diagram for the Fe-C System

Phase diagrams represent phase transformation and possible microstructures in alloys within a given temperature and a given composition, assuming equilibrium state and following the principle of minimum free energy. In this report, the binary diagram of Fe-C (Figure 1) will be enough for studying some alloys. Different types of alloying elements have different effects on the phase diagram according to Maalekian [2].

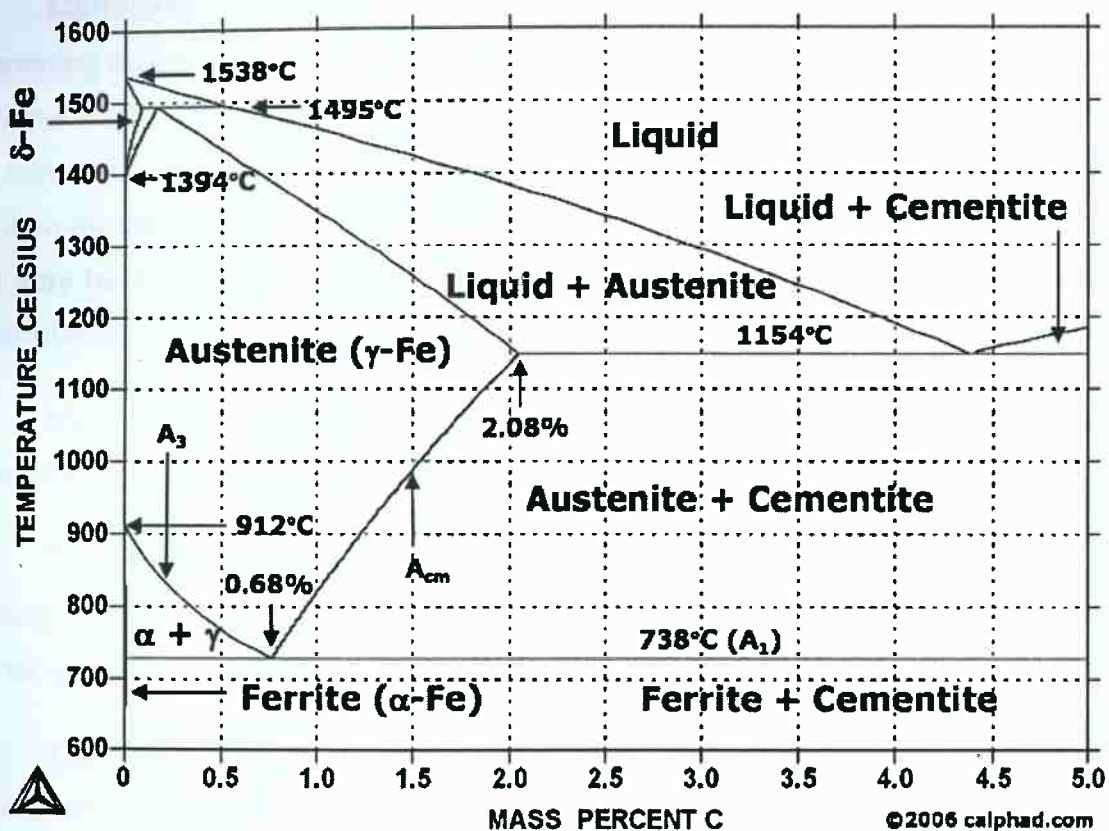


Figure 1 – Fe-C phase diagram at different temperatures. Source: [3].

For most of the steels, the Fe-C diagram is the basis for phase transformation. As shown in Figure 1, there are several temperatures which are very relevant for studying the behaviour of steel with specific Carbon contents at each temperature. In low carbon steel, thus the iron-rich portion of the diagram, there are three important temperatures concerning to phase transformation. They are the A₁, A₃ and A_{cm} temperatures, which represent the eutectoid reaction, the ferrite/austenite transformation and the austenite/cementite transformation, respectively. The letter 'A' stands for arrests and it is often accompanied by the scripts 'e', 'c' or 'r', which

represents the conditions of the transformation, whether it is under equilibrium, during heating ("chauffant") or during cooling ("refroidissant"), respectively.

Since the Fe-C phase diagram is only a guide for phase transformations under equilibrium conditions (although it can be used for even very complex alloys), studying steels must consider processing conditions and its effects on the microstructures.

3.1.2 Martensite Transformation

Martensite is a shear (or displacive) solid-state transformation originated by quenching austenite to room temperature. It is diffusionless since it can be formed at very low temperatures in which atoms don't have enough energy to diffuse, and it has the same chemical composition as the parent austenite. Therefor the carbon in solid solution remains in solution after the phase transformation. In other words, martensite is a very hard phase generated by a specific deformation of the austenite. To avoid other phases, such as perlite and ferrite, the cooling rate must be high enough [1].

Martensite also occurs in many types of materials besides steels, such as ceramics, polymers and nonferrous alloys.

The temperature in which the martensite transformation begins during rapid cooling is called the martensite-start temperature (M_s). The temperature in which martensite transformation reaches 95% is called martensite-finish (M_f).

The Eq. 1, known as the Koistinen-Marburger equation, relates the volume fraction of martensite with the M_s temperature [4].

$$1 - V_{\alpha'} = \exp\{\beta(M_s - T_q)\} \quad \text{Eq. 1}$$

$V_{\alpha'}$ is the volume fraction of martensite transformed when undercooling below M_s , which is the martensite-start transformation temperature. The quenching ends at a final temperature $T_q < M_s$. Normally T_q is set to be the room temperature. $\beta \approx -0.011$

The Koistinen and Marburger equation shows that martensite transformation is not time dependant.

3.1.3 Bainite Formation

Bainite is a displacive and diffusional transformation product of austenite. Its microstructure is basically formed by two phases, ferrite and cementite, in other words carbides aggregated to plate-shape ferrites. Bainite is nucleated preferentially at the austenite grain boundary and at temperatures between the M_s (martensite-start temperature) and the pearlite formation temperature.

This type of microstructure can be divided into two morphologies: upper bainite and lower bainite. The first appears as aggregates of ferrite laths almost parallel one to another and is formed at temperatures just below the pearlite start temperature. Upper bainite usually appears in the optical microscope as a feather-shaped structure nucleated from the austenite grain boundaries, coarse cementite precipitates from the carbon-rich austenite between the ferrite laths. While lower bainite is formed at temperatures that are just above M_s , it has an acicular appearance in optical microscope due to its ferrite plates, typically oriented at 60° within the plate axis, with fine cementite precipitates, which is responsible for high strength and toughness. [5]

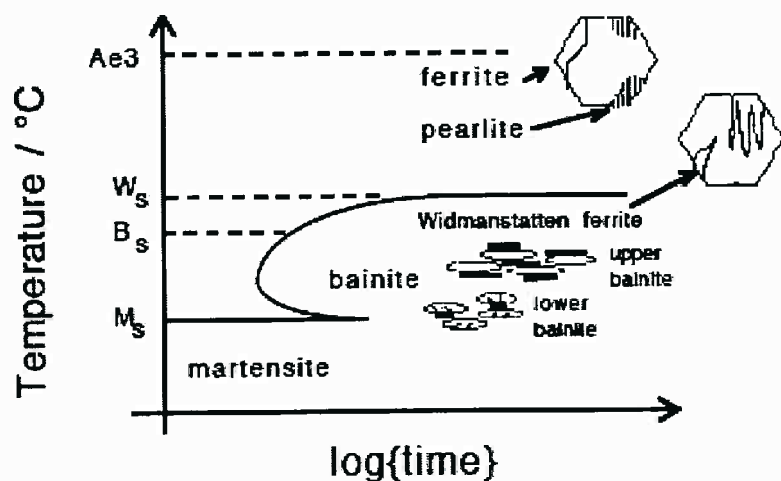


Figure 2 – TTT curves showing the different domains of transformation. Source: [5].

3.1.4 Tempering of bainite

Unlike in martensite, the concentration of carbon in solid solution of bainite is little, since in the latter case coarse carbides are formed between ferrite plates. In general, tempering martensite attempts to remove – precipitate – dissolved carbon,

consequently lowering its strength. However, tempering bainite does not alter significantly its strength due to the small quantities of dissolved carbon. Nevertheless, some minor change in strength can be observed because of the coarsening of cementite particles. Also, retained austenite in bainitic microstructures can decompose into ferrite + carbides when tempering at temperatures above 400°C.[1]

3.2 ALLOYING ELEMENTS IN STEELS

3.2.1 Substitutional elements

Using the allotropic forms of iron as basis for phase transformation in steel, the addition of other elements may form substitutional BCC and FCC solid solutions. As they replace the iron atoms at first, they can then be called as substitutional alloying elements. These atoms are approximately the same size as the iron atom [1].

The substitutional elements can be divided in two categories: alfa stabilizers and gamma stabilizers. The first stabilizes the bcc structure of the iron (ferrite), e.g. Chromium and Molybdenum. While the latter stabilizes the FCC structure of the iron (austenite), e.g. Manganese and Nickel.

3.2.2 Interstitial elements

For the same allotropic forms of iron, if smaller size atom elements are added, they may take places of some iron atoms inside the crystal structures, i.e. in their interstices, forming interstitial solid solutions.

Concerning steels, the most important interstitial elements are Carbon and Nitrogen. Ferrite has very low solubility for interstitial elements since it has small interstitial sites in the BCC form. On the other hand, austenite has larger interstices in the FCC form and thus it has greater solubility for interstitial elements.

The different solubility of Carbon in austenite and ferrite can explain some phase transformations in steel. When it is heated to austenite stable temperatures, carbon should dissolve thru the interstices, and when cooled down to ferrite stable temperatures, carbon must leave the structure. Depending on the cooling rate different structures might be formed.

If cooled slowly, ferrite will begin to be formed and the carbon concentration in austenite will increase forming carbides. If cooled very quickly, i.e. quenched, the BCC structure will be supersaturated, and other structures will be formed.

The alloying elements can be divided into two groups:

- Carbide-forming elements, e.g. Cr, Mn, V, Ti and Nb
- Non carbide-forming elements, e.g. Ni, Si, Al and Cu.

The first group of elements can be divided again into carbides that do not compete with cementite (e.g. Ni, Si and Mn), strong carbide-forming elements (e.g. Mo, Cr and W) and even stronger carbide-forming elements (e.g. Nb, Ti and V). The second group elements do not interact with carbon and iron and thus they remain in solid solution with iron. Although at low temperatures Cu dissolves in Fe [Malakian].

3.2.3 Microalloying in steels

Some strong carbide-forming elements are well known as microalloying elements notably because very low additions of these elements can change several properties in steels such as strength, toughness, and weldability. They are mainly used for grain refinement and precipitation strengthening in High Strength Low Alloy (HSLA) steels [1].

Some of these elements, such as Nb, are also known to have a solute drag effect, hindering the interface mobility during the $\gamma \rightarrow \alpha$ transformation. It is possible that the same effect occurs during the $\alpha \rightarrow \gamma$ transformation as well, either as solid solution or as precipitates. This effect is responsible for delaying bainite formation.

When fine NbC precipitate they become an obstacle for grain boundaries mobility, this way the grain growth is hindered by grain boundaries that are pinned. In metallurgy this effect is known as pinning effect.

3.2.4 Transformation Diagrams

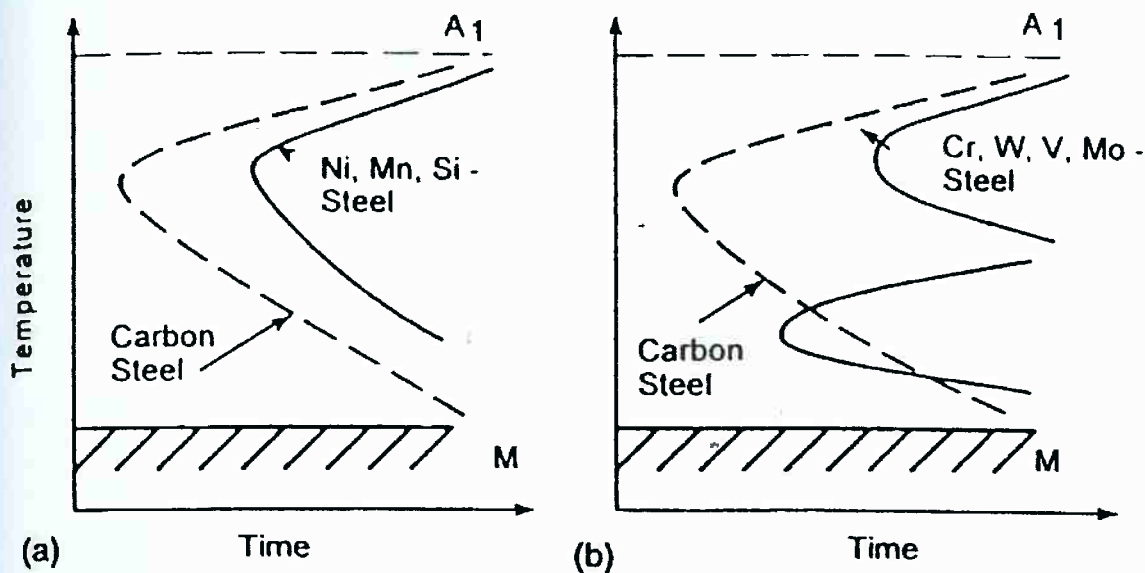


Figure 3 – Diagrams of isothermal transformation: (a) Carbon steel and steel alloyed with non-carbide-forming elements; (b) carbon steel and steel alloyed with carbide-forming elements [5].

3.2.5 Effect on TTT curves

The isothermal transformation diagrams in Figure 4 show the effect of increasing amounts of Mn on the cooling rates for transformations to occur. Therefore, it is noticed that increasing concentration of Mn leads to a delay on transformation beginning, since Mn lowers the A1 temperature and thus widens the austenite field.

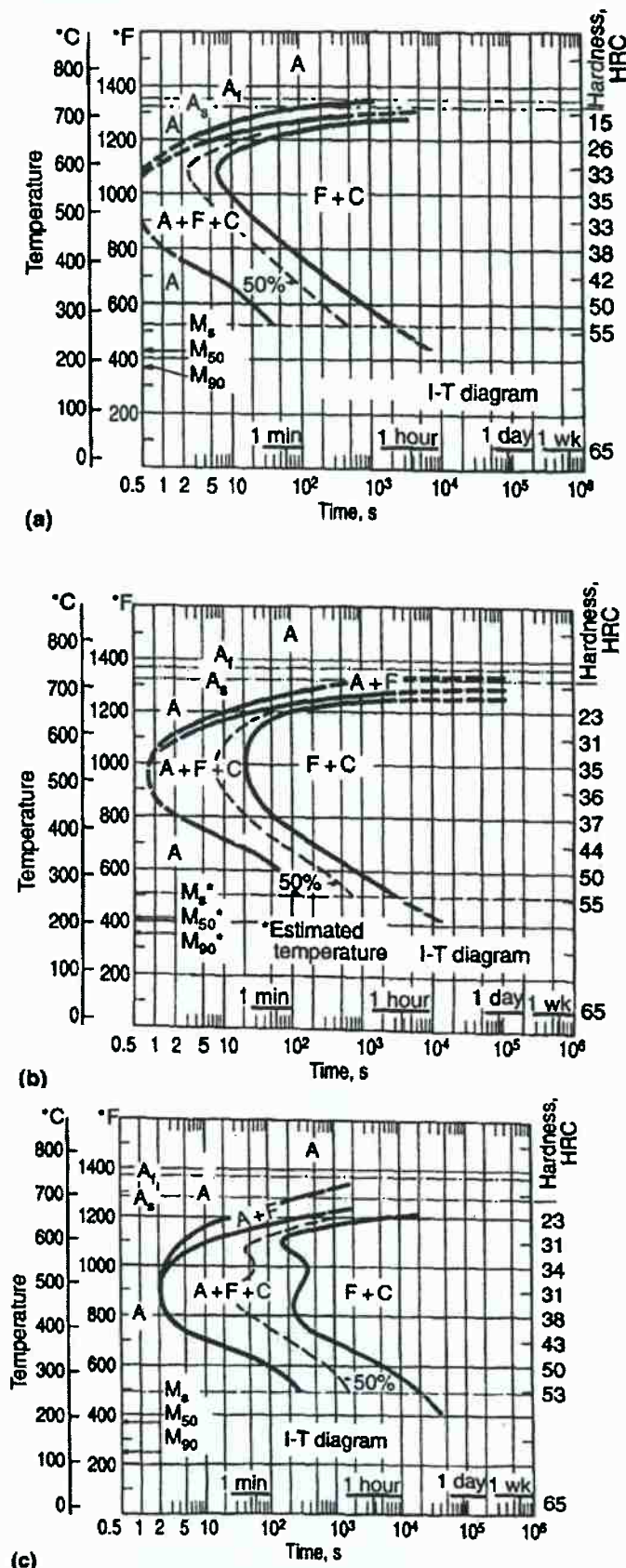


Figure 4 – isothermal transformation diagrams showing the effect of increasing amounts of Mn on the cooling rates. Source: [6].

The precipitation of carbides and nitrides of these elements occurs at different temperatures and can be related to their solubility products. As shown in Figure 5, the solubility of carbide increases with increasing temperature. The effectiveness of these carbides will depend on their distribution and fineness. The driving forces for this are mainly the interfacial energy between the current phase and the carbide and the crystal arrangements of the compounds.

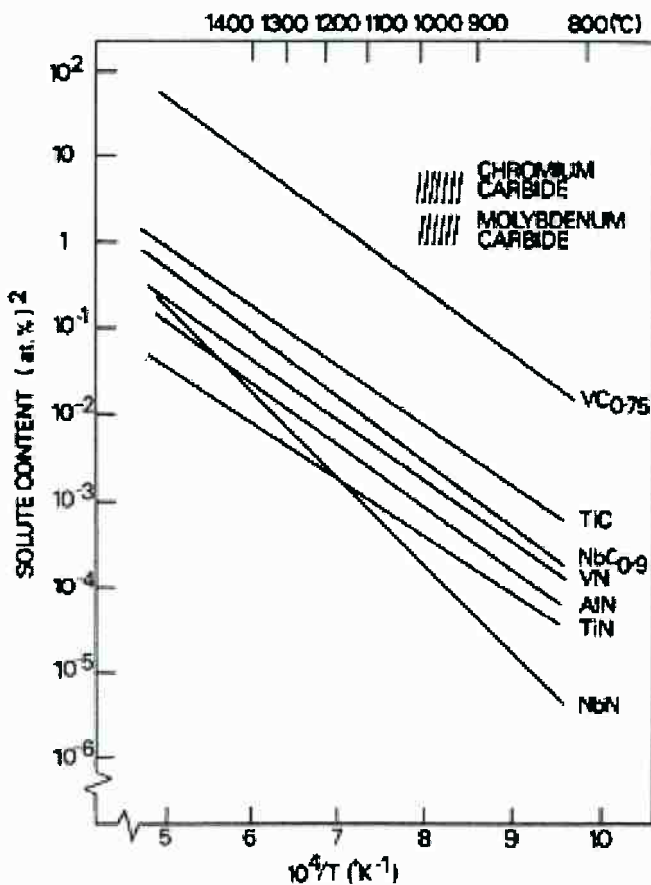


Figure 5 – Solubility product of carbides and nitrides in austenite as a function of temperature [7]

3.3 HIGH STRENGTH STEELS (HSS) AND ADVANCED HIGH STRENGTH STEELS (AHSS)

HSLA steels have yield strengths greater than 275 MPa (lower yield strengths are considered mild steels). In general, they have a ferrite/perlite composition in the initial stage, i.e. before going through any metallurgical transformation process.

Despite the many discussions between researchers around a clear definition of HSLA steels, it is quite unanimous that essentially it implies microalloyed steels.

Therefore, one can say that HSLA steels contain in addition to some alloying elements -e.g. Manganese, Silicon and Aluminum – very low quantities of microalloying elements – e.g. Niobium, Vanadium and Titanium. The HSLA steels are mainly applied in structural and construction purposes, such as oil and gas pipelines, high rise buildings and automobile components [1].

4 CHOOSING THE COMPOSITION

To investigate the effect of Mn and its γ stabilizing property, different contents of Mn were chosen to be studied. Furthermore, Nb was added to some compositions to study how Mn affects Nb dissolution which, in fact, is showed to be a positive effect of enhancing NbC solubility in austenite as Figure 6 from Koyama et al [8]. It was also possible to study the potential of precipitating as Nb-rich particles.

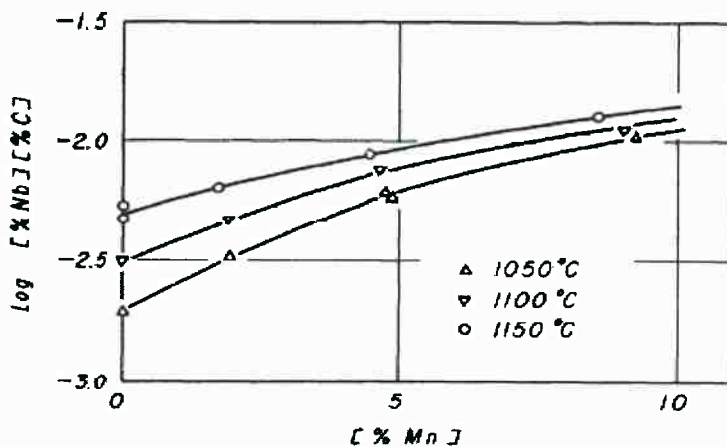


Figure 6 – Effect of Mn on the solubility product of NbC in austenite. Source: [8].

Figure 7 shows Koyama's calculations for different Mn contents the amount of Nb that can be put into solution depending on the reached temperature. It is noticed that for temperatures up to approximately 1250°C, increasing amounts of Mn increase Nb in solution, which can be up to approximately 600ppm.

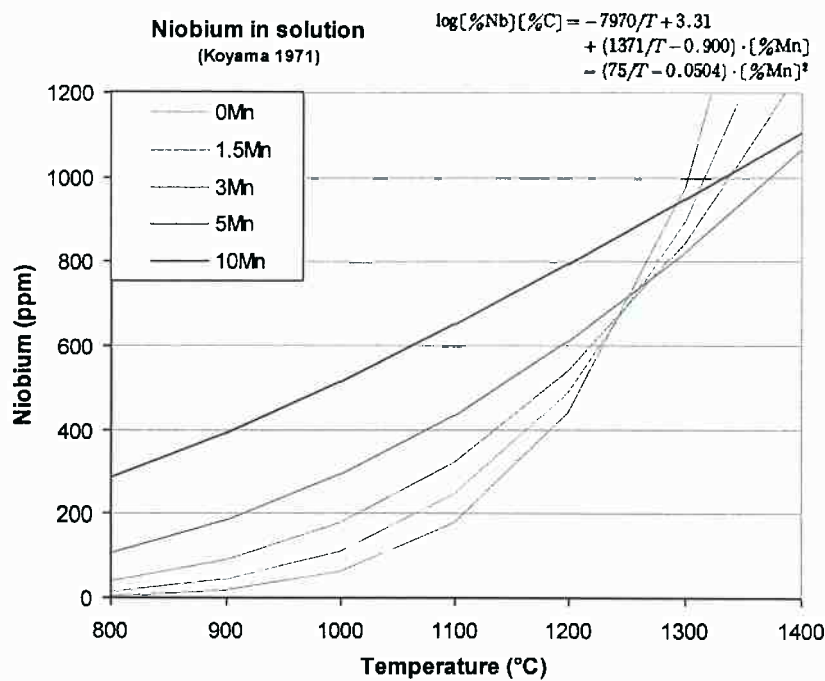


Figure 7 – A3 Influence of Mn solubility of NbC in austenite. Soure: [8].

Si, on the other hand, as an α stabilizer, decreases Nb solubility. Fig illustrates this effect. Another effect that is associated to Si is to prevent cementite precipitation, allowing carbide-free bainite to form and thus improving toughness. Compositions with and without Si were chosen to investigate the effect of Si. However regarding the effect of Si when added to a Mn alloyed steel. Liu [9] studied Mn and Si influences on bainite transformation and found that Mn alone and Si alone have very different roles between each other and also different from when Mn and Si are combined.

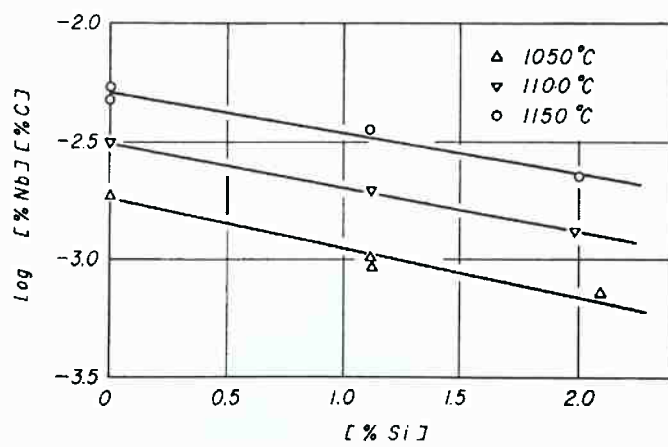


Figure 8 – Effect of Si on the solubility product of NbC in austenite. Source: [8].

5 MATERIALS AND EXPERIMENTAL METHODS

5.1 MATERIALS

Table 1 shows the chemical compositions made in the Arcelor Mittal casting facility. Ingots of 15kg each were casted in vacuum induction melting furnace. No homogenization treatment was programmed. The ingots were divided in four parts and one part was hot rolled and air cooled from 900°C down to a coiling temperature of 400°C along with their respective reference names.

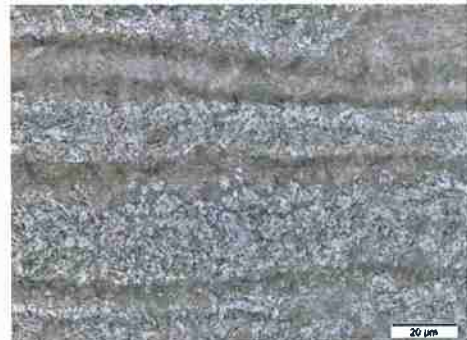
Table 1 – Chemical compositions of samples

	Reference	Composition (wt%)			
		C	Mn	Nb	Si
1,5%Mn	2217A	0,18	1,5	0	0
	2217B	0,18	1,5	0	1,5
	2340A	0,18	1,5	0,1	0
	2340C	0,18	1,5	0,1	1,5
3%Mn	2475A3	0,167	2,95		
	2475B3	0,167	2,97	0,047	
	2475C3	0,167	2,96	0,1	
	2475D3	0,167	2,91	0,99	1,65
5%Mn	2468A3	0,173	5,08		
	2468B3	0,174	4,99	0,049	
	2468C2	0,168	4,92	0,091	
	2468D2	0,168	4,89	0,106	1,79

Hot rolled samples in the condition "as received" were polished in diamond suspension up to $1\mu\text{m}$ following standard metallographic analysis specimen preparation and etched with Nital 2%. The pictures below are the observations made in a Light Optical Microscope.



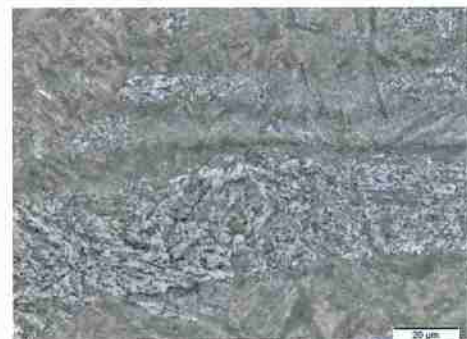
a



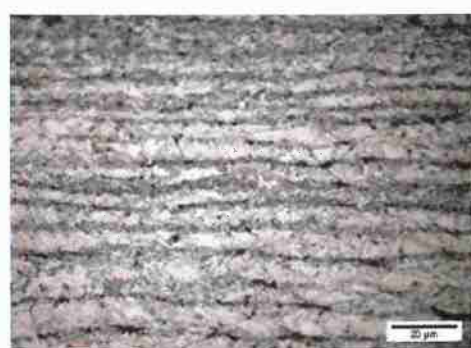
e



b



f



c



g

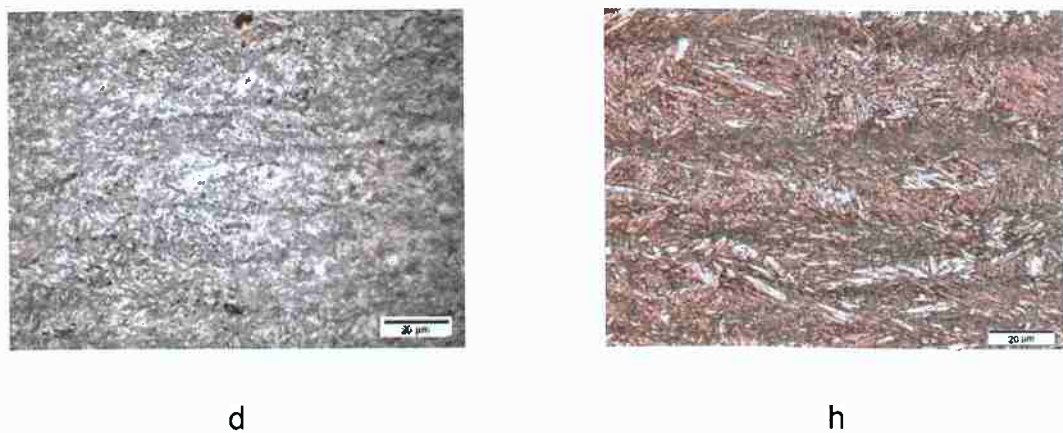


Figure 9 – (a-d) 3Mn (Nital) and (e-h) 5Mn (Picral + Metabisulfite) with 0Nb, 0.05Nb, 0.1Nb and 0.1Nb-1.5Si. Additions of Mn avoid ferrite and pearlite formation during air cooling after hot rolling. Si additions increases more hardenability.

5.2 EXPERIMENTAL METHODS

Dilatometer specimens measuring 10mm x ϕ 4mm and 10mm x 4mm x 4mm were submitted to different thermal cycles in a Bähr 805 dilatometer. The temperatures of the cycles were controlled by thermocouples that were welded on the middle of the sample, this latter was held by hollow push rods that measured the samples change in length. All cooling steps were performed by helium gas valve systems.

The austenitizing temperature was chosen to be 1250°C for sufficient time as 300s to assure high Nb dissolution, although it is known that high temperatures and long austenitizing periods also result in larger austenite grain sizes. After austenitizing, the samples followed the steps described in sections 4.2, 4.3 and 4.4.

Some samples were observed in optical microscope following standard metallography procedures and etched with Picral and Metabisulfite 4%. Other samples were only used for data reproduction.

One sample of each composition was held during 5 minutes at 1250°C and quenched to room temperature (Figure 10). The cooling rate applied for quenching in all the thermal cycles in this study was approximately 50°C/s.

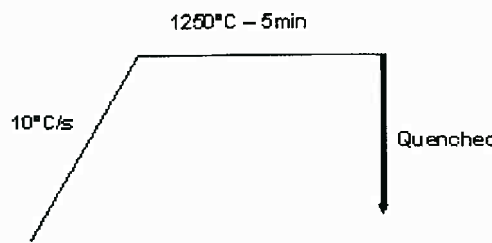


Figure 10 – Thermal treatment cycle: Austenitizing at 1250°C for 5 minutes followed by Quenching (~50°C/s)

5.2.1 Ferrite to Austenite transformation: Ac_1 and Ac_3 temperatures

Dilatometric curves were analyzed to determine the ferrite to austenite transformation start and finish temperatures (Figure 11) during heating.

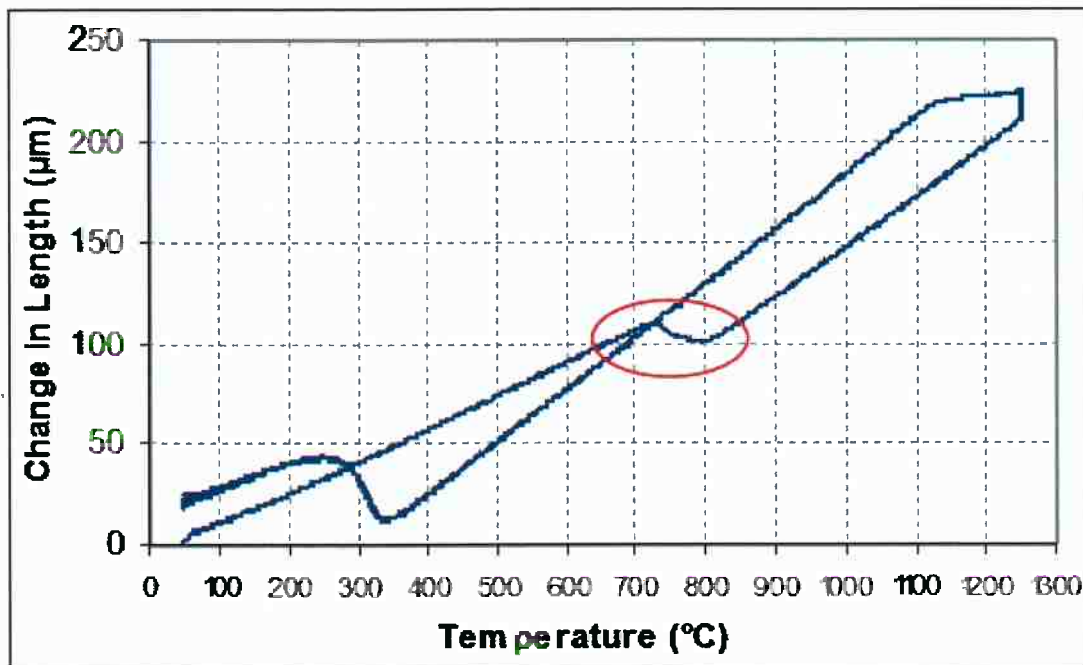


Figure 11 - Ferrite to Austenite transformation during heating in a dilatation curve

Approximate tangent lines were traced at the beginning and at the end of the transformation (Figure 12). It is supposed that when the curve deviates from the first tangent line it will represent the beginning of the ferrite to austenite transformation. Hence when the curve reaches the second tangent line it will represent the end of the $\alpha \rightarrow \gamma$ transformation.

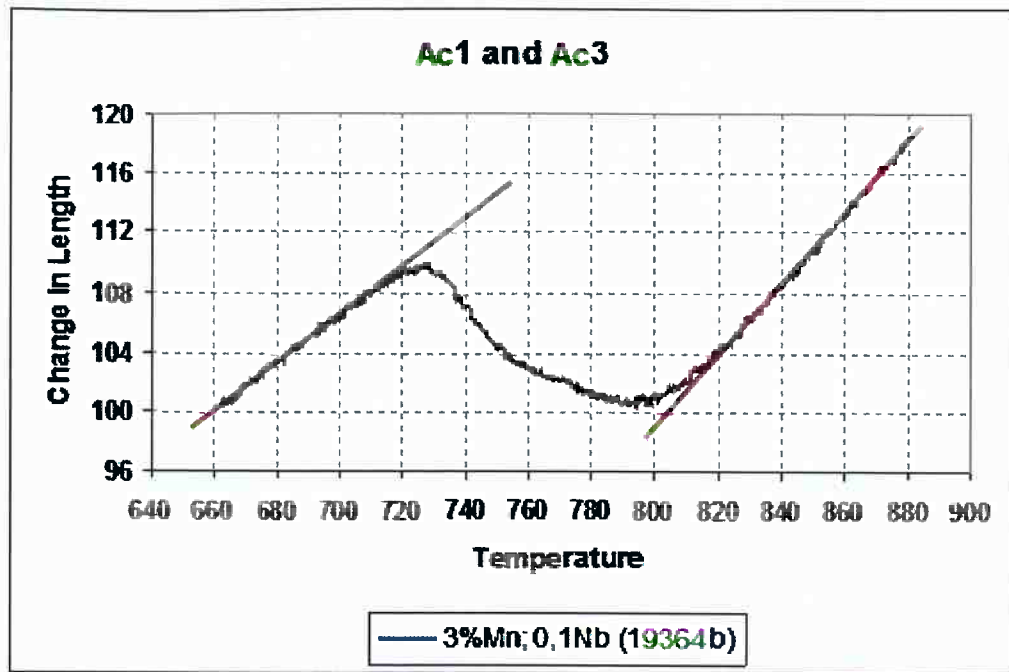


Figure 12 - Tangent lines traced at the beginning and at the end of $\alpha \rightarrow \gamma$ transformation

5.2.2 Martensite transformation: Ms temperature.

Martensite start temperature was obtained from the dilatometric curves upon cooling, when specimens were quenched to room temperature (Figure 13).

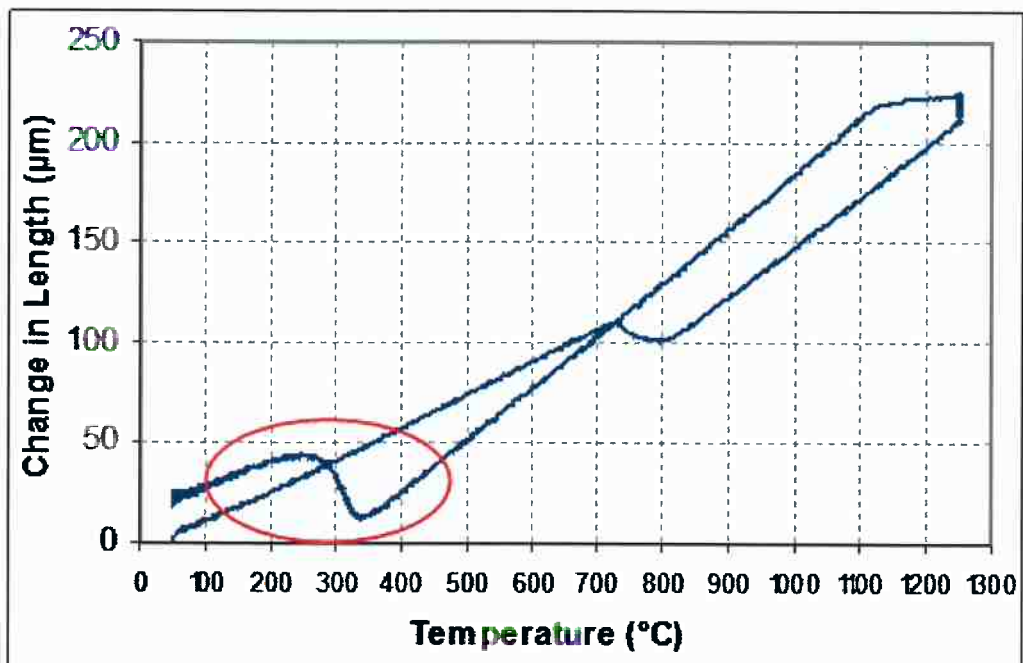


Figure 13 - Martensite transformation during quenching in a dilatation curve.

Two tangent lines are plotted on the martensite transformation portion of the curve (Figure 14). At the beginning of the transformation it is assumed that 0% of martensite is formed (pink tangent line=y1), while at the end of transformation it is assumed that 100% is formed (red tangent line=y2).

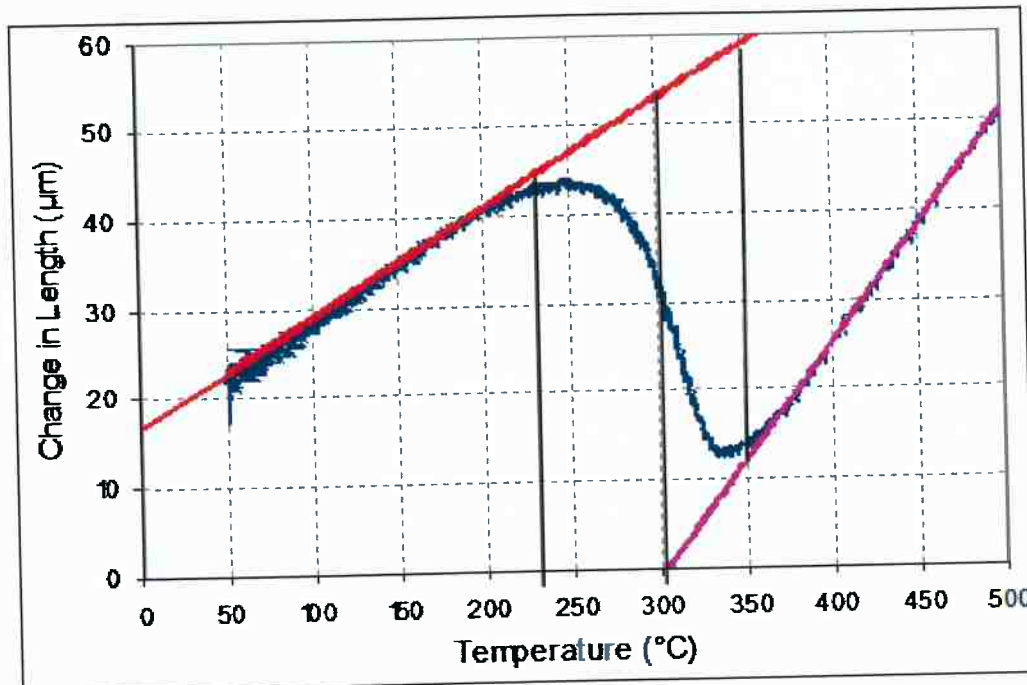


Figure 14 - Tangent lines at the beginning and at the end of Martensite transformation.

Equation 2 describes the lever rule applied to the sequence in which martensite transformation occurs:

$$V_f = (y_1 - f(T)) / (y_1 - y_2) \quad \text{Eq. 2}$$

Where V_f is the Martensite volume fraction, $f(T)$ is the dilatometric curve, and y_1 and y_2 are tangent lines to $f(T)$ immediately before and after the transformation happens respectively.

The martensite volume fraction was plotted as a function of the temperature during cooling for each test (Figure 15).

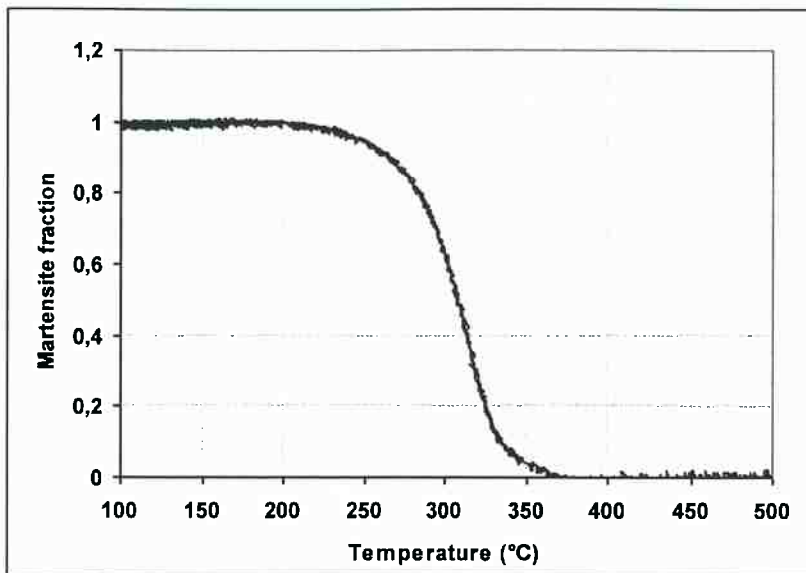


Figure 15 – Graph showing the Martensite volume fraction as a function of Temperature during Martensite transformation upon quenching.

5.2.2.1 Koistinen & Marburger method to determine Ms1

Equation 1, prescribed by Koistinen and Marburger [4], calculates the martensite volume fraction in terms of the martensite start temperature and the temperature during the transformation upon cooling.

$Vf(K-M)$ is plotted as a function of the temperature during transformation and fitted to the volume fraction graph (Figure 15) from Equation 1. This fitting is illustrated in **Erro! Fonte de referência não encontrada.**. $Ms1$ is assumed as the point where $Vf(K-M)=f(T)$ intersects the X-axis.

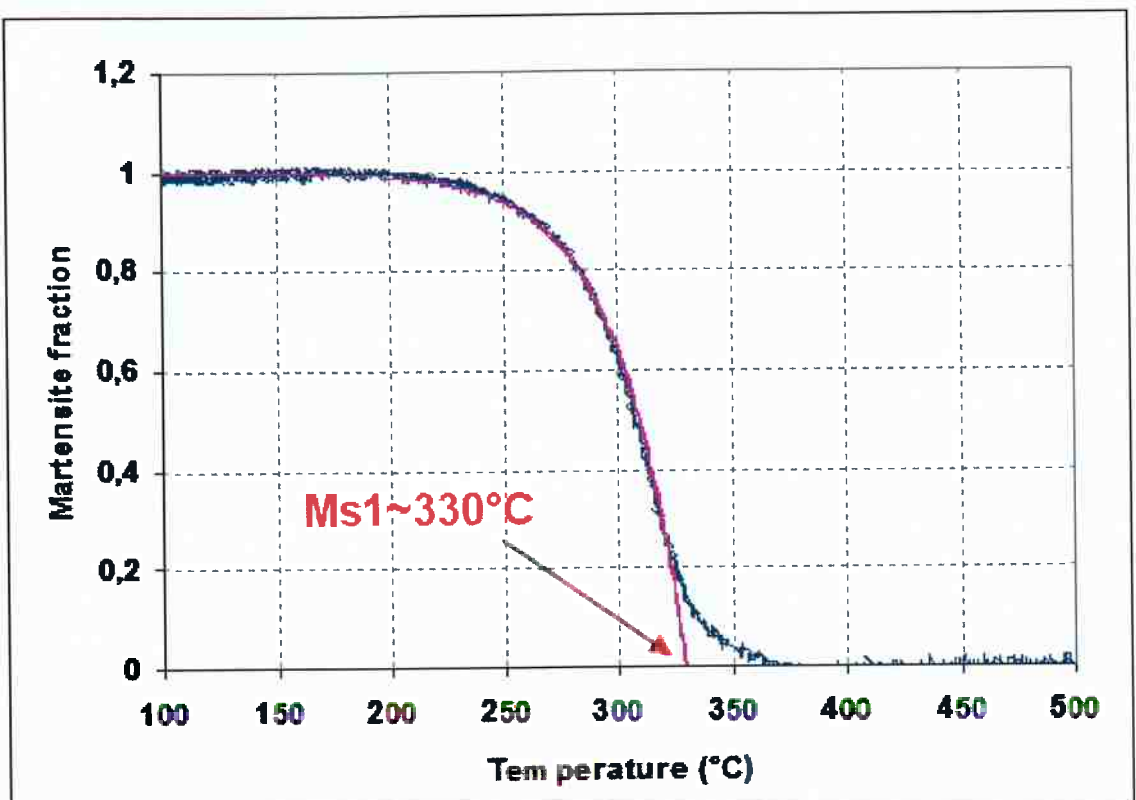


Figure 16 - Koistinen & Marburger fitted to transformed Martensite Volume fraction for Ms1 estimation.

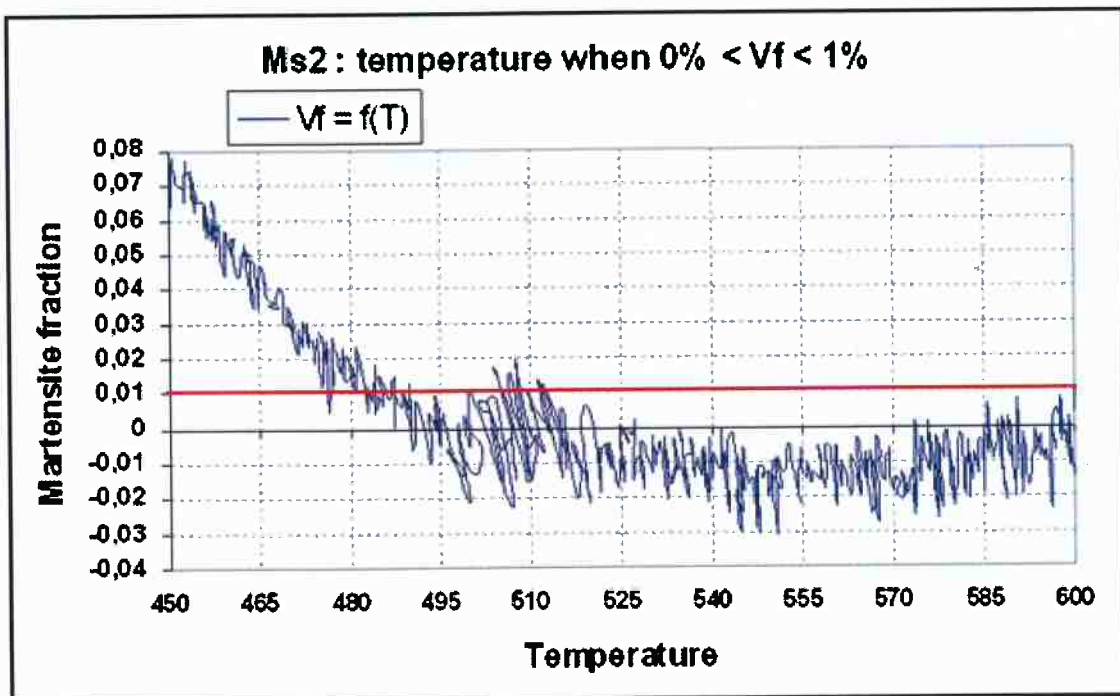


Figure 17 - Graph illustrating Ms2 estimation.

5.2.3 Bainite formation

Initially the bainite formation temperature was intended to be $Ms_1 + 10^\circ C$. But when samples were quenched down to such isotherms, martensite was formed instead of bainite. Even $Ms + 30^\circ C$ was not sufficient to obtain bainite.

Thus, it was chosen to work with $400^\circ C$ as an isothermal temperature for the samples with no Si, since Si allows lower bainite formation temperatures. This temperature was chosen based on previous investigations from Cobo et al. [10].

3%Mn samples with different Nb concentrations were submitted to a thermal cycle of austenitizing at $1250^\circ C$ for 5 minutes followed by quenching to $400^\circ C$, held isothermally for 5 minutes and quenched to room temperature (Figure 18).

A composition with Si was held at $365^\circ C$ ($Ms + 30^\circ C$) and was compared to one without Si held at $400^\circ C$ ($Ms + 70^\circ C$).

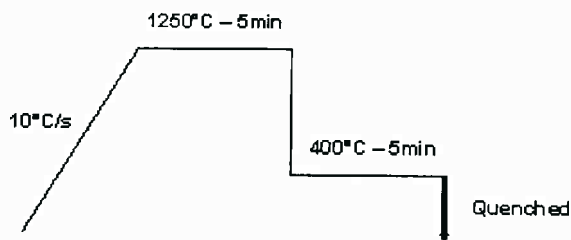


Figure 18 – Thermal cycle for bainite formation.

Specimens were observed by light optical microscope after standard metallographic procedures. Furthermore, Vickers hardness test was applied to each specimen.

5.2.4 Tempering of bainite

Austenitized, isothermally held at $400^\circ C$ (*) for 5 minutes and tempered at $600^\circ C$ for different times: 6 minutes, 1 minute and 30 seconds (Figure 19).

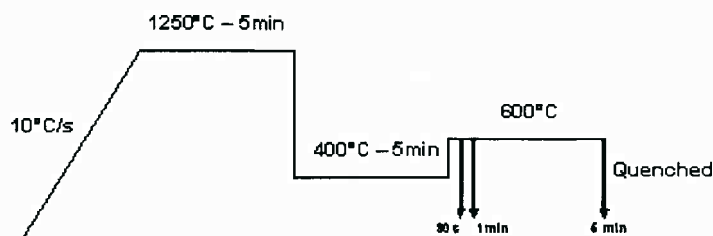


Figure 19 – Bainite tempering cycles

Specimens were observed by light optical microscope after standard metallographic procedures. Furthermore, Vickers hardness test was applied to each specimen.

6 RESULTS AND DISCUSSION

The table below shows the values for Ac₁, Ac₃, Ms₁ (Ms) and Ms₂ for each sample. Ms₂ was only estimated for the 3%Mn samples since these it was chosen to be the initial composition for bainite formation and furthermore NbC precipitation in tempered bainite.

Table 2 - Experimentaly estimated Ac₁, Ac₃, Ms (Ms₁) and Ms₂ values for each s valu for each composition.

SAMPLES		Ac ₁	Ac ₃	Ms	Ms ₂
2217 (1,5% Mn, 0Nb)	A	728	846	363	
	B		916	370	
2340 (1,5% Mn/0,1% Nb)	A	734	873	340	
	C	735**	927	359	
2475 (3% Mn)	A3	704	802	324	385
	B3	716	809	327	365
	C3	717	821	329	375
	D3	720**	897	307	355
2468 (5% Mn)	A2	682	742	245	
	B2	690	757	261	
	C2	693	771	277	
	D2	700**	875	260	

6.1 EFFECT ON AC1 AND AC3

The transformation zone extracted from the dilatation curves for samples 2217A, 2475A3, 2468A2 during heating up to 1250°C (Figure 20) shows that increasing concentrations of Mn lead to decreasing Ac1 and Ac3 temperatures. It also narrows the transformation gap. In industry this would mean lower austenitizing temperatures and therefore a gain of time.

Mn as a γ -field opening element is expected to widen the austenite field by lowering the $\alpha \rightarrow \gamma$ transformation temperature and rising it for $\gamma \rightarrow \delta$. Thus, both austenite transformation beginning (Ac1) and finish (Ac3) are lowered by adding sufficient amounts of Mn.

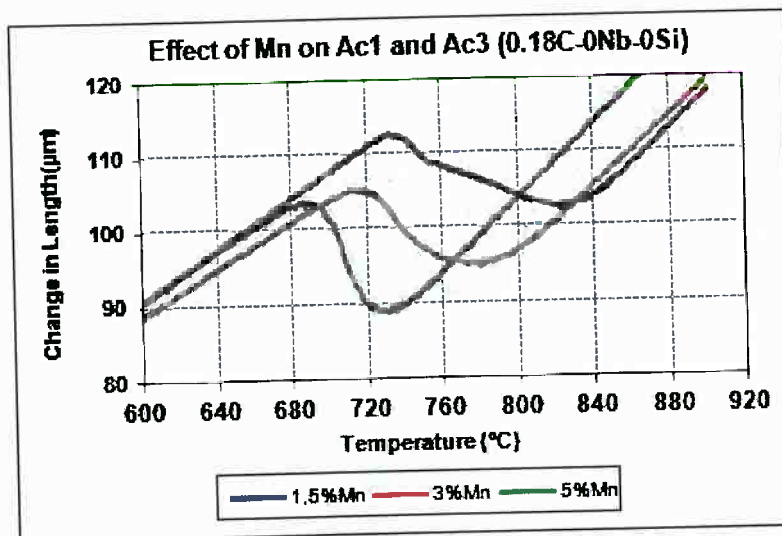


Figure 20 – The effect of different concentrations of Mn on Ac1 and Ac3.

Figure 21 shows the effect of Si on heating critical temperatures, despite to what is known for the Si as an α stabilizer, it seems to widen the $\alpha \rightarrow \gamma$ transformation field, slightly increasing the Ac3 temperature.

Figure 22 shows how Mn affects critical temperatures when adding Si (1.5%). Liu [9] studied the effect of Si when combined with Mn, and his studies concluded that Si seems to enhance Mn segregation to austenite grain boundaries, increase the carbon content in austenite, decreasing the bainitic α nucleation rate, i.e. it turns out

to delay transformations from prior austenite. This could probably explain the γ -field be favoured during $\alpha \rightarrow \gamma$ transformation.

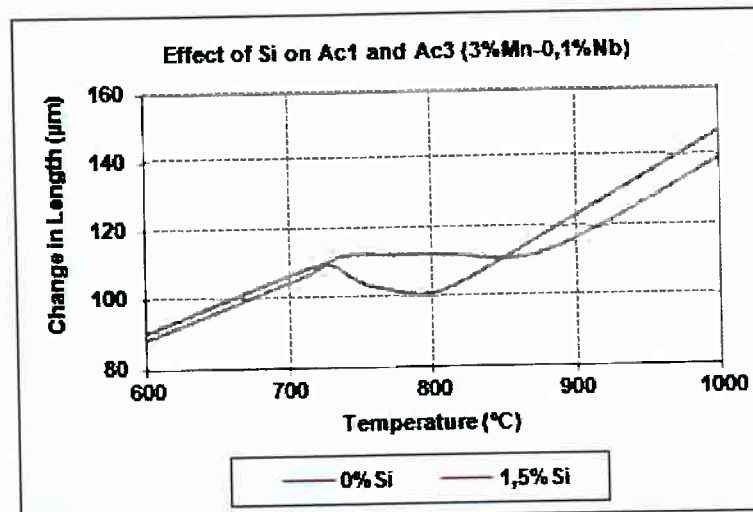


Figure 21 – The effect of different amounts of Si on Ac1 and Ac3.

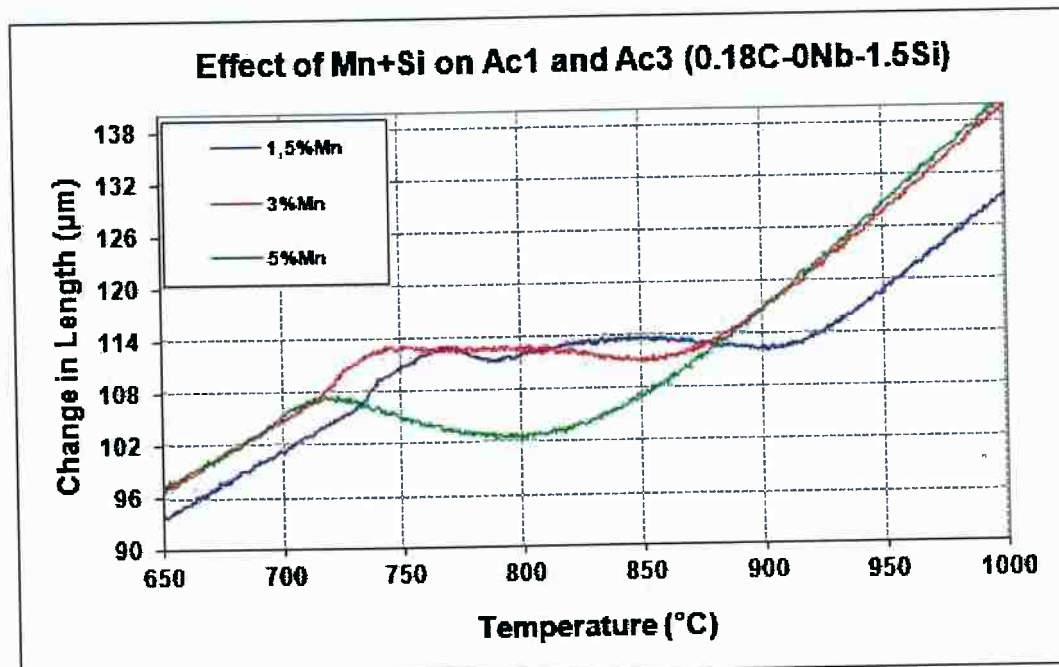


Figure 22 – The effect of different concentrations of Mn on 0%Nb-1.5%Si samples.

Figure 23 is an overview of the effects of Mn, Nb and Si (Si+Mn effect). As seen before, Mn lowers the critical temperatures and narrows the transformation range. It seems that Nb additions slightly increase Ac1, whereas the same effect is more evident for Ac3. It also appears that Si has a considerable effect on widening the austenite transformation range, especially by increasing Ac3. Therefore, when it comes to Si addition it is important to define whether the $\alpha \rightarrow \gamma$ transformation range is

the priority, which could mean a wider working range, i.e. favouring the control of phase volume upon transformation, or whether it is desired to quickly reach austenitzing temperatures furthermore to achieve rapidly a martensite structure.

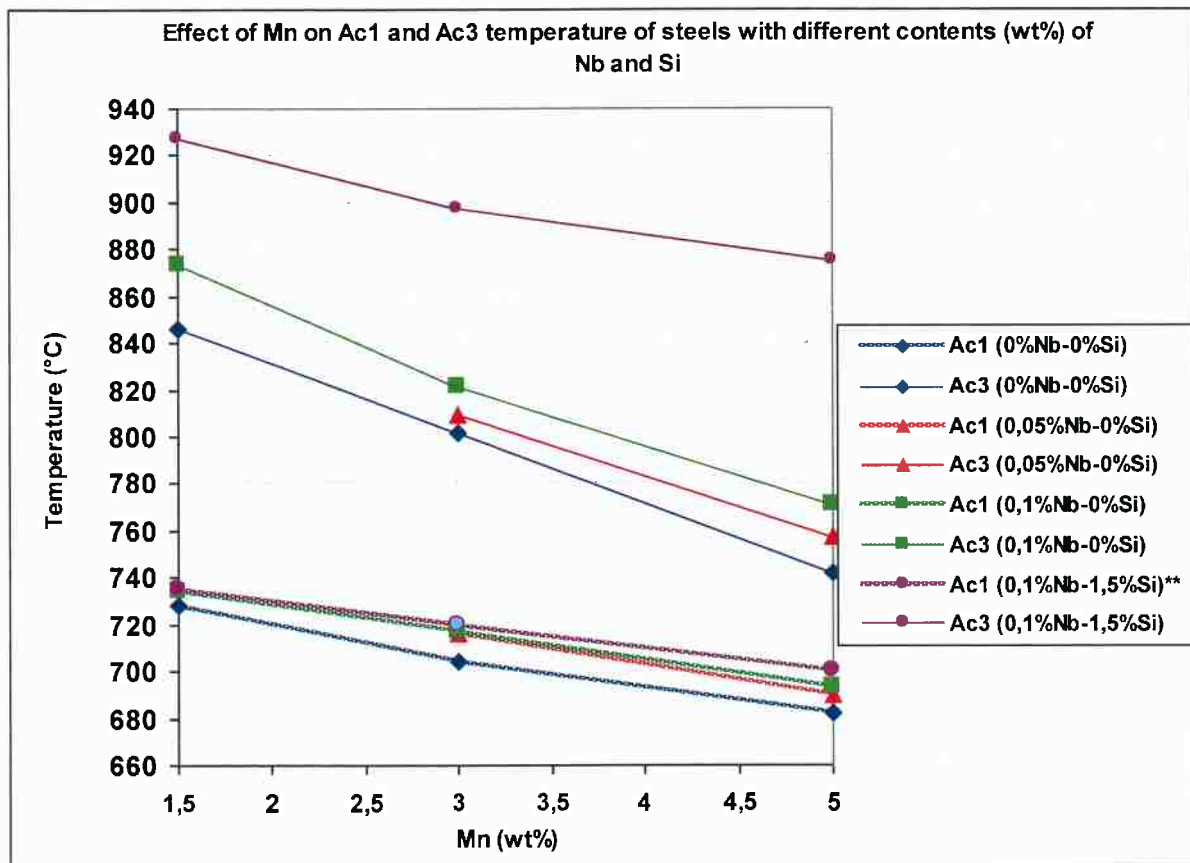


Figure 23 – The effect of Mn on critical temperatures, Ac1 and Ac3, of samples that vary in Nb and Si concentrations.

6.2 EFFECT ON MS1

Figure 24 compares the calculation of martensite start temperatures proposed by different authors and the Ms1 obtained experimentally in this study. Each author described the influence of the alloying elements in different ways. Nevertheless, the main compounds in all three equations are carbon and manganese. Some elements were removed from the equations since they are not present in the composition of the samples studied in the present work.

$$Ms = 512 - 453C + 217(C)^2 - 71.5 C Mn \quad \text{Eq. 3 [11]}$$

$$Ms = 545 - 330C - 23Mn - 4Nb - 7Si$$

Eq. 4 [12]

$$Ms = 539 - 423C - 30.4Mn - 7Si$$

Eq. 5 [13]

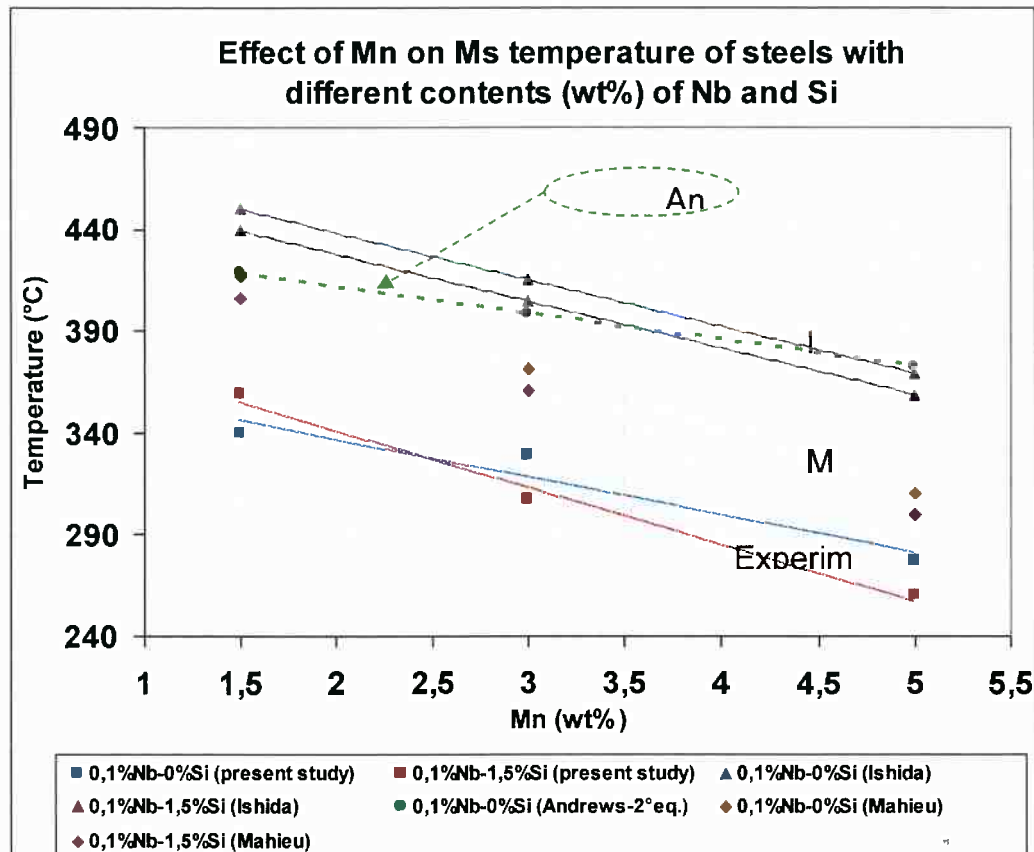
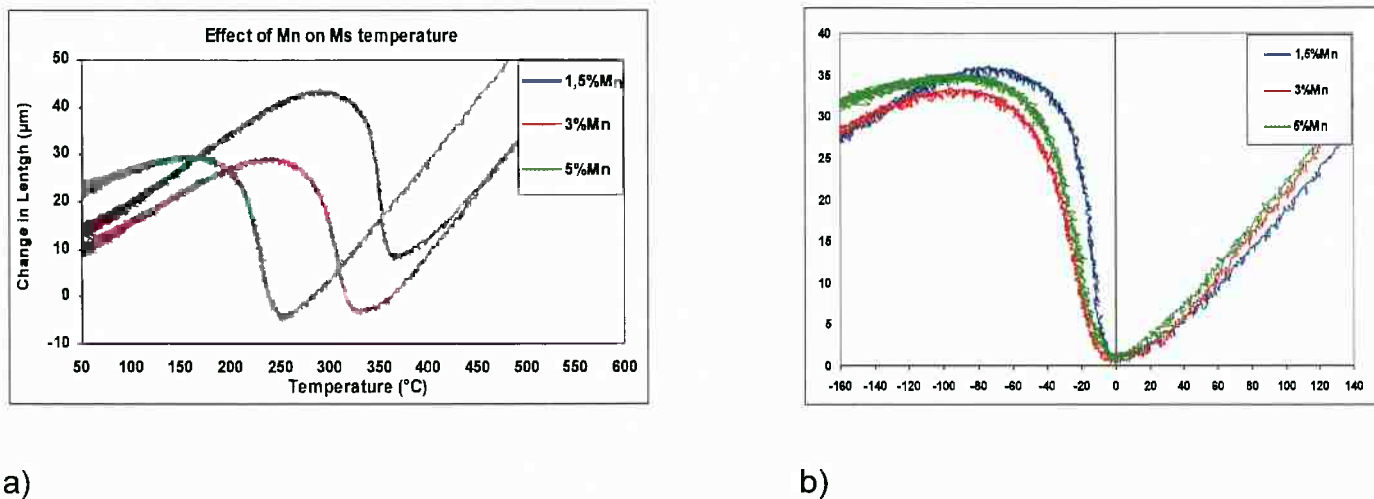


Figure 24 – A comparison of the effect of Mn on Martensite-start temperature (Ms) with different Si concentrations in 0.1%Nb samples calculated by using 4 distinct methods : the present study, Andrews, Ishida, and Mahieu.

Figure 25 shows the curves obtained from the dilatometer from which Ms was graphically found for samples varying in Mn concentration.



a)

b)

Figure 25 – Dilatometry curves during martensite transformation for different contents of Mn.
a) Effect of Mn on the Ms temperature; b) Effect of Mn on the kinetics of transformation.

The graph below shows how the Ms1 behaves differently with different amounts of alloying elements. Three important effects can be noticed straight away:

Mn lowering the Ms temperature, i.e. martensite transformation is retarded by increasing Mn contents.

Figure 26 shows the effect of Mn on Ms with increasing Nb contents, in which Ms is lower for higher Nb contents at 1.5% Mn and goes towards the opposite sense as Mn increases.

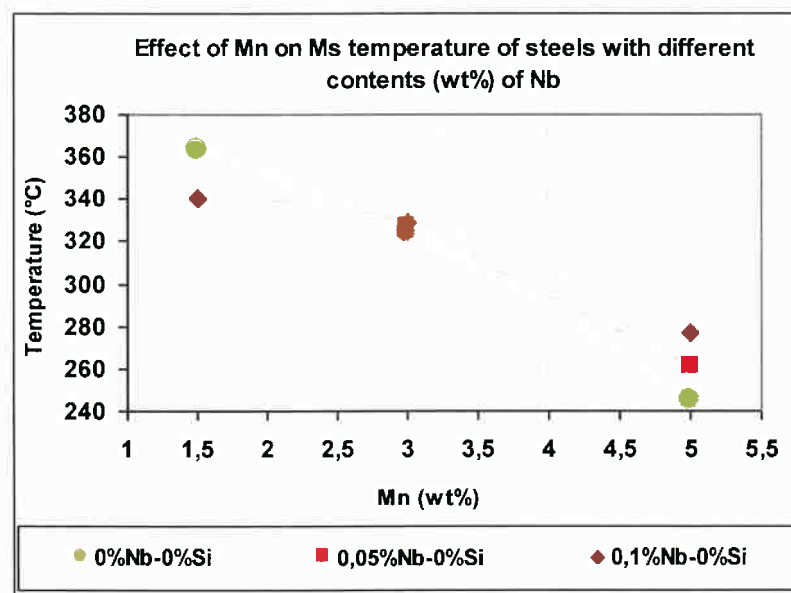


Figure 26 – The effect of Mn on the Ms of samples with different Nb concentrations.

Xiuqiu [14] found in his studies that Mn increased NbC dissolution in temperatures between 1100°C and 1250°C. Still NbC particles only disappeared in electron microscope observations when Mn contents were enough as 2.18%. Figure 26 and Figure 27 confirm that Nb contents do in fact influence differently when changing the Mn concentration. The first evidences that indeed around 2.5%Mn there is a switch between the curves with and without Nb. While the latter shows more clearly that Mn has an important influence on the role of NbC particles.

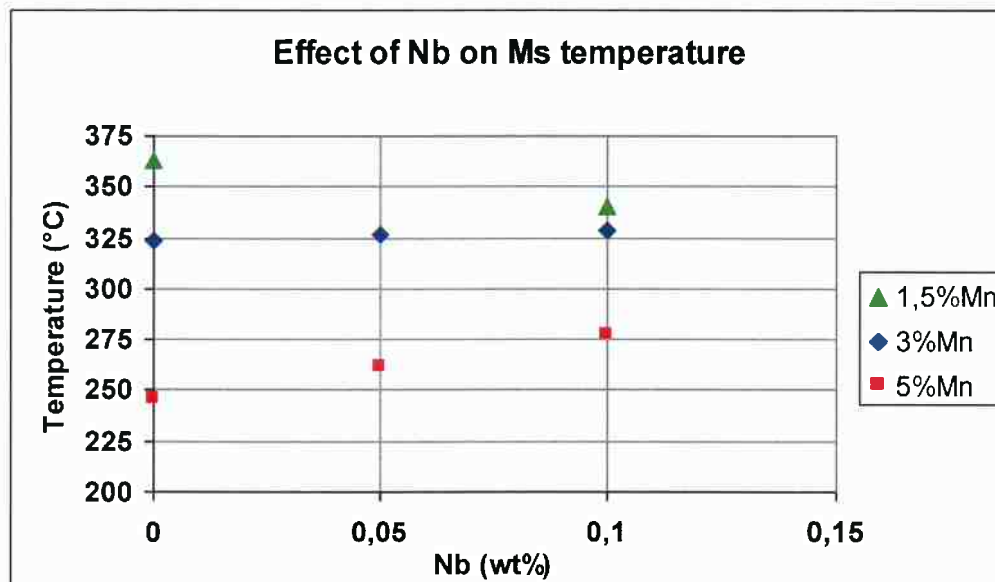


Figure 27 – The effect of Nb on the Ms of samples with different Mn concentrations.

Figure 28 below shows the curves obtained by using the dilatometer from which Ms was graphically found for samples varying in Nb concentration. It confirms that, Nb concentrations do not have a significant influence on samples that contain 3% Mn.

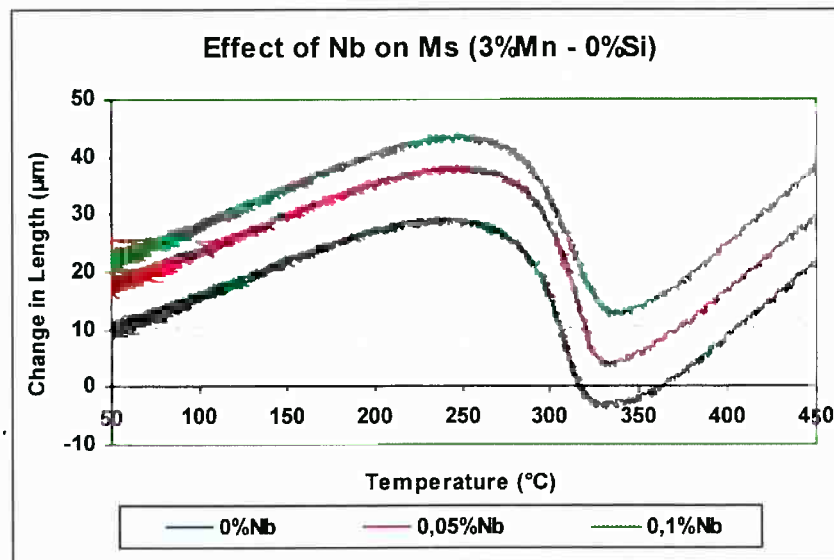


Figure 28 – Dilatometry curves during martensite transformation for different contents of Nb in samples with 3% Mn-0% Si.

However, different concentrations of Si seem to slightly affect the Ms in 3% Mn samples as demonstrated in Figure 29.

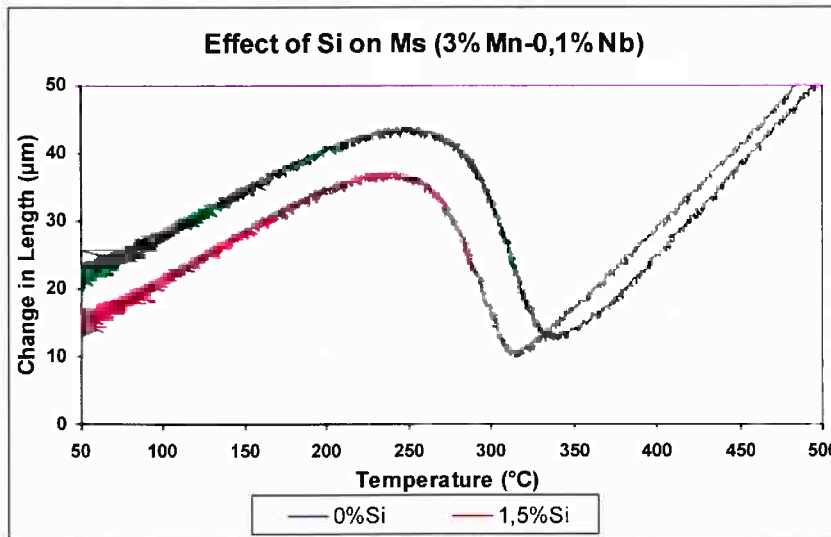


Figure 29 – Dilatometry curves during martensite transformation for different contents of Si in samples with 3% Mn-0.1% Nb.

Figure 30 and Figure 31 show in two different graphic models how Ms is affected by both Mn and Si contents variations. Adding Si lowers Ms in samples with 3% Mn and 5% Mn, but actually it happens when Mn concentrations overcome 2%

(more or less). When Mn concentration is below 2%, Si has the opposite effect, increasing Ms.

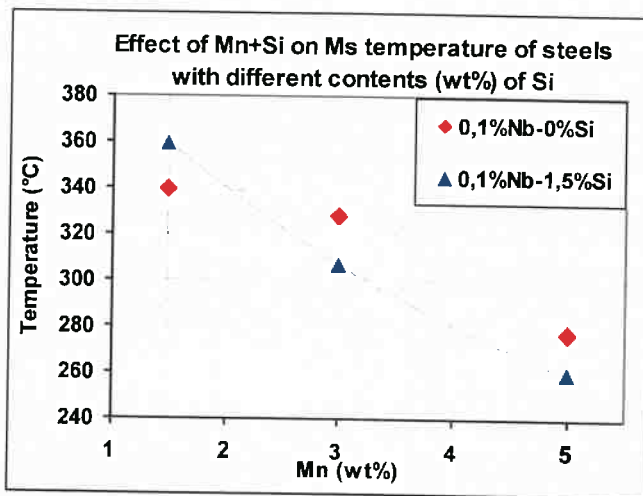


Figure 30 – The effect of Mn on the Ms of samples with different Si concentrations.

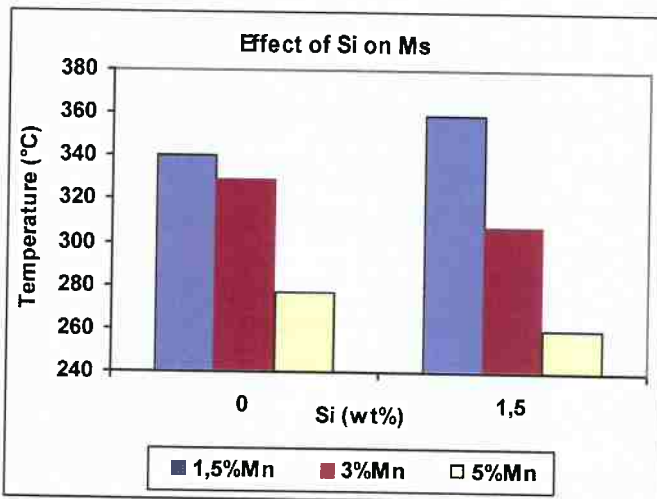


Figure 31 – A column graphic showing the effect of Mn on the Ms of samples with different Si concentrations.

6.3 ON BAINITE FORMATION

6.3.1 Bainite Kinetics

By holding bainite formation at 400°C for different periods of time – 30", 1' and 6' – it was found that bainite achieves its completion after 200" for samples without Si. However, it took more than 300" to finish bainite formation in the sample containing 1.5%Si. Bainite completion wasn't even finished after 360" (6'). So it was considered

that 300" of bainite formation would be adequate to compare all of the 4 samples through the same cycle.

According to Liu [9], Si might have an important role on delaying the bainite nucleation rate in C-Mn steels since it increases Mn segregation at austenite grain boundaries which makes it difficult for Fe₃C to precipitate, thus keeping the γ phase rich in C and hindering the transformation. His study also confirmed that this is an important effect of Si when combined with Mn. Each element separately should have different effects on the kinetics.

Regarding to compositions containing 3%Mn, Nb showed to no significant effect on Ms. Consequently, Nb had small effects on the bainite formation kinetics as well. As for the Si, the bainite formation is remarkably retarded when compared to the same samples without Si, even though it was isothermally held at a temperature much closer to Ms.

Figure 32 below shows an important influence of Si on retarding the bainite formation, whereas increasing contents of Nb doesn't seem to have any great contribution to the kinetics of the bainite formation

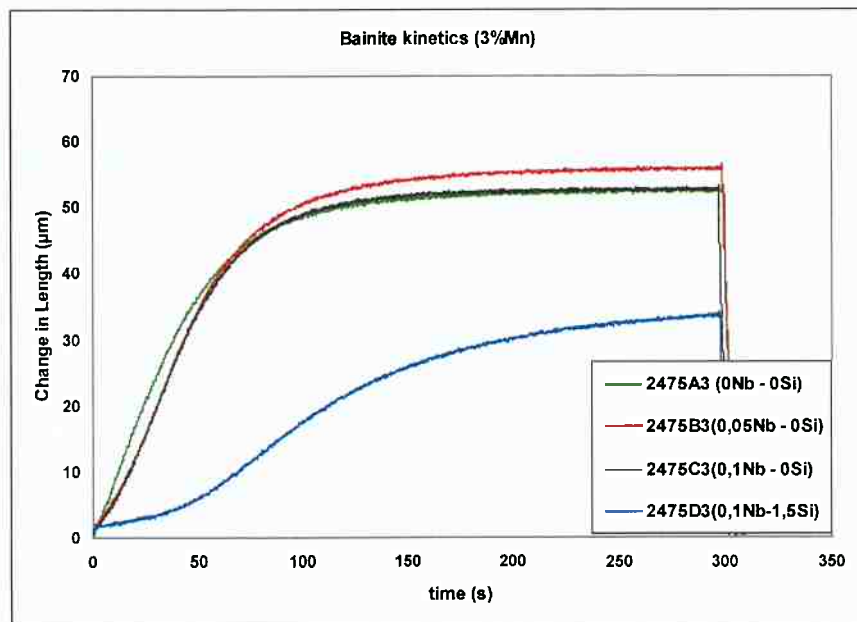


Figure 32 – The effect of different Nb and Si concentrations on bainite formation kinetics. Samples were austenitized for 5 minutes and quenched to 400°C for bainite formation, and quenched again to room temperature after 5 minutes.

Before tempering at 600°C, it was chosen to hold samples isothermally at 400°C for 300" (5') to guarantee bainite completion in all 4 samples.

6.3.2 Microstructure of the bainite

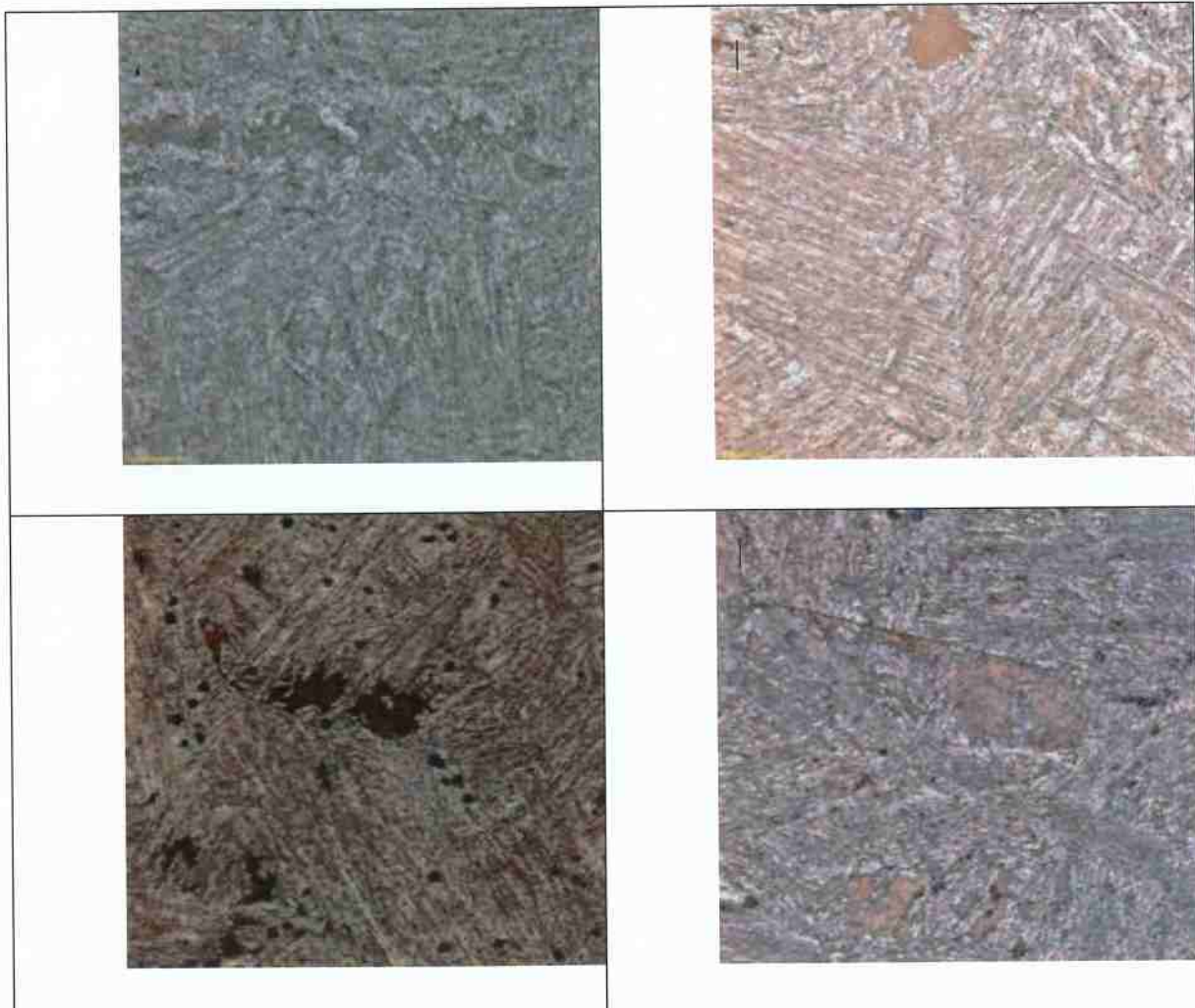


Figure 33 – Microstructures of 3Mn-0.18C-(0-0.1)Nb-(0-1.5)Si. Samples were austenitized at 1250°C, isothermally treated at 400°C for 5 min and quenched. Picral followed by Metabissulfite etching. A) 0Nb-0Si; B) 0.05Nb-0Si; C) 0.1Nb-0Si; D) 0.1Nb-1.5Si

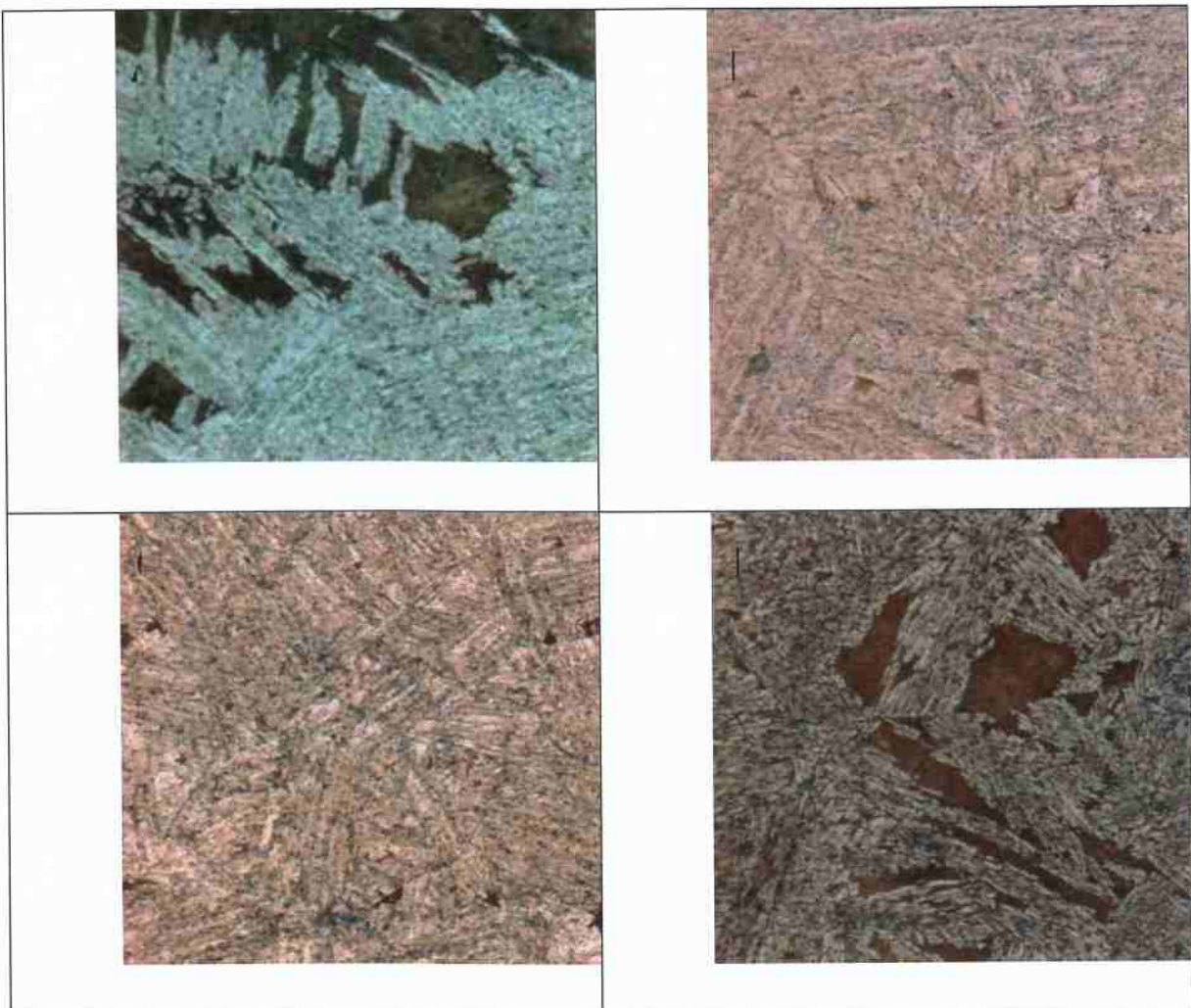


Figure 34 – Microstructures of 3Mn-0.18C-(0-0.1)Nb-(0-1.5)Si. Samples were austenitized at 1250°C, isothermally treated at 400°C for 5 min, tempered at 600°C for 5 min and quenched. Picral followed by Metabissulfite etching. A) 0Nb-0Si; B) 0.05Nb-0Si; C) 0.1Nb-0si; D) 0.1Nb-1.5Si

6.3.3 Vickers hardness test

Figure 35 shows that hardness is increased with Nb additions, but hardly changed with different tempering times. By adding Si hardness is significantly enhanced. However, short tempering periods seemed to be more effective on hardness increasing than longer periods of tempering. Nevertheless, the composition with Si did not reach complete bainite formation, therefore it is expected to obtain higher values for hardness since the untransformed austenite resulted in martensite after quenching.

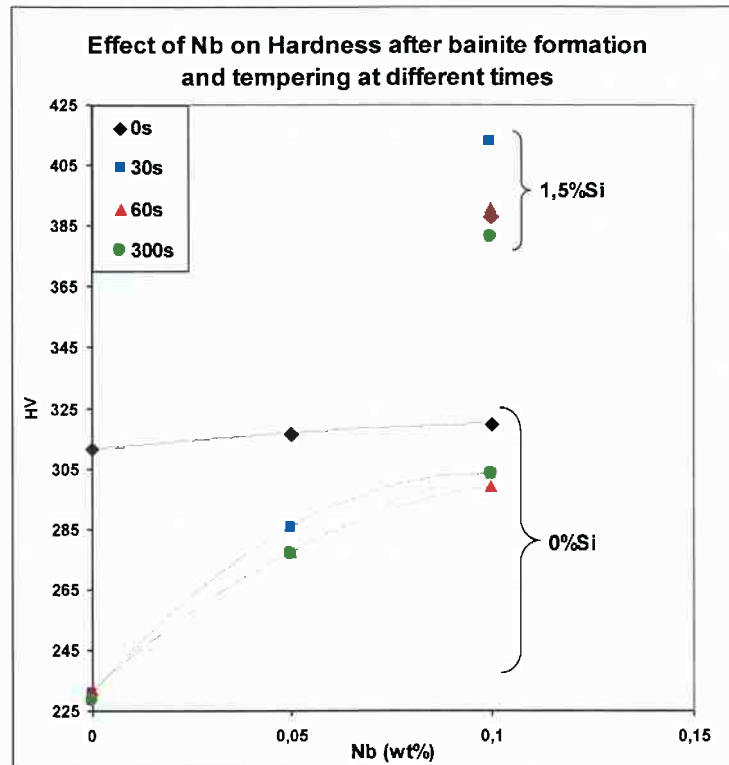


Figure 35 – The effect of Nb and Si additions on Vickers Hardness measured after bainite formation at 400°C/5' and tempering at 600°C for different periods of time : 30", 60" and 300". The 0" curve represents the samples that were quenched right after bainite formation at 400°C/5'.

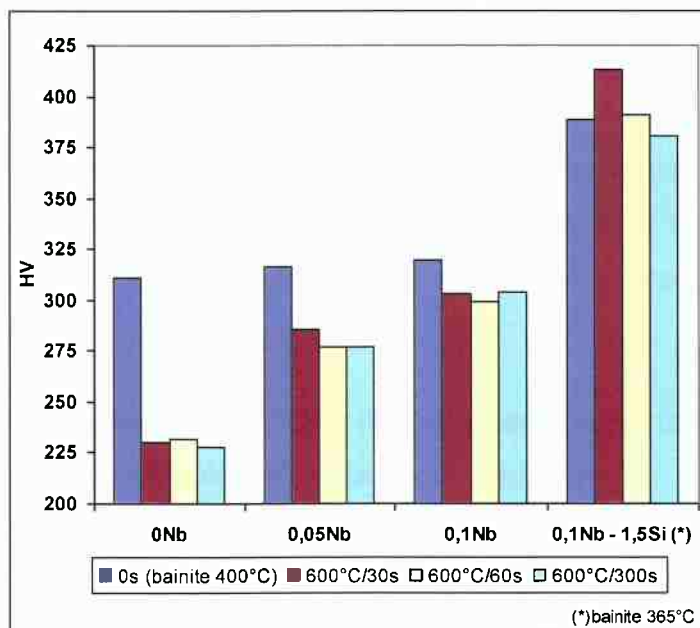


Figure 36 – Graphic with columns showing the effect of Nb and Si additions on Vickers Hardness measured after bainite formation at 400°C/5' and tempering at 600°C for different periods of time : 30", 60" and 300". The 0" column represents the samples that were quenched right after bainite formation at 400°C/5'.

7 CONCLUSIONS

- Adding Mn allows working with lower austenitization temperatures. However, the binary phase range is considerably narrowed which will compromise the precision to control phase fractions.
- It is believed that Mn enhances the Nb dissolution in austenite by segregating at austenite grain boundaries, this way hindering ferrite nucleation in these sites.
- Ms was lower for higher Nb contents in 1.5%Mn samples and went towards the opposite sense as Mn concentration was increased.
- Adding Si lowers Ms in samples with more than 2%Mn. When Mn concentration is below 2%, Si has the opposite effect, increasing Ms
 - Si slows down the bainite nucleation kinetics by increasing Mn segregation at austenite grain boundaries which makes it difficult for Fe₃C to precipitate, thus keeping the γ phase rich in C and hindering the transformation.
 - It was possible to achieve satisfactory Hardness level in tempered bainite when increasing Nb concentration, but the tempering times do not seem to affect significantly.
 - Si addition showed an important increase on Hardness. But it should be expected since bainite formation did not reach completion in this study, allowing martensite transformation during quenching. Nevertheless, short tempering times seemed to be more effective on samples with Si.
 - Further studies should aim finding the time elapsed for the bainite formation to be complete (or close to completion) in samples containing Si.

8 REFERENCES

1. BHADESHIA, H.; HONEYCOMBE, R. **Steels: Microstructure and Properties.** [s.l: s.n.].
2. MAALEKIAN, M. **The Effects of Alloying Elements on Steels (I).** [s.l: s.n.].
3. CALPHAD. **Metastable iron-carbon (Fe-C) phase diagram.** Disponível em: <<http://www.calphad.com/iron-carbon.html>>.
4. KOISTINEN, D. P.; MARBURGER, R. E. A general equation prescribing the extent of the austenite-martensite transformation in pure iron-carbon alloys and plain carbon steels. **Acta Metallurgica**, v. 7, n. 1, p. 59–60, 1959.
5. BHADESHIA, H. K. D. H. **Bainite in steels.** 2^a ed. London: IOM Communications LTD, 2001.
6. ASM INTERNATIONAL. HANDBOOK COMMITTEE. **ASM handbook.** [s.l: s.n.].
7. PORTER, D. A.; EASTERLING, K. E. **Phase Transformations in Metals and Alloys, Third Edition (Revised Reprint).** [s.l.] CRC Press, 1992.
8. KOYAMA, S.; ISHII, T.; KIICHI, N. **Effects of Mn, Si, Cr and Ni on the Solution and Precipitation of Niobium Carbide in Iron Austenite.** J. Japan Inst. Metals, 1971.
9. LIU, S. K.; ZHANG, J. The influence of the Si and Mn concentrations on the kinetics of the bainite transformation in Fe-C-Si-Mn alloys. **Metallurgical Transactions A**, v. 21, n. 6, p. 1517–1525, 1990.
10. COBO, S. et al. **Precipitation of Nb(C,N) in the temperarure range 450-600°C in low carbon bainitic steels.** [s.l: s.n.].
11. ANDREWS, K. W. Empirical formulae for the calculation of some transformation temperatures. **Journal of Iron and Steel Institute**, v. 203, n. 7, p. 721–727, 1965.
12. ISHIDA, K. Calculation of the effect of alloying elements on the M s

temperature in steels. **Journal of Alloys and Compounds**, v. 220, n. 1, p. 126–131, 1995.

13. MAHIEU, J. et al. Phase transformation and mechanical properties of {Si-free CMnAl TRIP}-aided steel. **Metallurgical & Materials Transactions A**, v. 33, n. August, p. 2573–2580, 2002.

14. XIUQIU, L.; WENXUAN, C. The effect of manganese on the recrystallization of austenite in low-carbon niobium steels. International Conference on HSLA Steels. **Anais...** Beijing: 1985